12-2016

# Exploring the Production of Extracellular Matrix by Astrocytes in Response to Mimetic Traumatic Brain Injury

Addison Walker
*University of Arkansas, Fayetteville*

Exploring the Production of Extracellular Matrix by Astrocytes in Response to Mimetic Traumatic Brain Injury

A thesis submitted in partial fulfillment
of the requirements for the degree of
Master of Science in Biomedical Engineering

by

Addison Walker
University of Arkansas
Bachelor of Science in Biomedical Engineering, 2014

December 2016
University of Arkansas

This thesis is approved for recommendation to the Graduate Council.

_____
Dr. Jeff Wolchok
Thesis Director

_____
Dr. Kartik Balachandran
Committee Member

_____
Dr. Woodrow Shew
Committee Member

**Abstract and Key Terms**

Following injury to the central nervous system, extracellular modulations are apparent at the site of injury, often resulting in a glial scar. Astrocytes are mechanosensitive cells, which can create a neuroinhibitory extracellular environment in response to injury. The aim for this research was to gain a fundamental understanding of the affects a diffuse traumatic brain injury has on the astrocyte extracellular environment after injury. To accomplish this, a bioreactor culturing astrocytes in 3D constructs delivered 150G decelerations with 20% biaxial strain to mimic a traumatic brain injury. Experiments were designed to compare the potential effects of media type, number of impacts, and impacts with or without strain. Multiple impacts on astrocytes resulted in increased apoptosis, supporting cumulative effects of multiple traumatic brain injury events. Surprisingly, the expression of glial fibrillary acidic protein and S100B by astrocytes was downregulated following injury. With multiple impacts, astrocytes downregulated collagen and glycosaminoglycan expression at acute time points. Suppression of matrix metalloproteinase-2 coupled with unchanging production of transforming growth factor beta-1 and tissue inhibitor of metalloproteinase-1 indicates an inability to degrade damaged ECM or produce new ECM. This was supported by long-term studies which indicate significant decreases in chondroitin sulfate proteoglycan and collagen I accumulation. This could suggest astrocytes experiencing damaging mechanical stimulation enter a survival state ceasing to moderate the extracellular environment at short time points after injury.

Key terms: traumatic brain injury, astrocytes, extracellular matrix, glial scar, repeat injury

**Acknowledgements**

This work was supported by the National Science Foundation (Grant #CMMI-1404716) and the Arkansas Biosciences Institute. Special thanks is given to Joe Wyatt, Abby Terlow, and Nasya Sturdivant for assistance with cell culture and assays.

Special recognition is extended to Dr. Kartik Balachandran's lab and Dr. David Zaharoff's for generously allowing use of the lyophilizer, thermal cycler, and spectroscopy equipment.

**Table of Contents**

**List of Figures**



**Appendix Figures**

## I. Introduction

*Traumatic Brain Injury*

Traumatic brain injury (TBI) is described as an alteration of brain pathology caused by an external force (1). An estimated 1.7 million people in the U.S. experience a TBI annually, resulting in over 50,000 fatalities; however, the true number could be much larger as not all individuals that experience a TBI actively seek medical attention (2, 3). The incidence of TBI appears to have increased in recent years as TBI-related emergency department visits have increased 29% over a 5 year time span (4). The substantial proportion of the population affected by TBI creates an economic burden estimated to cost $63.4 billion to $79.1 billion from medical treatment and lost productivity (5).

TBI can be classified by a variety of parameters given the nature of the injury (blast injury, closed head injury) and the severity of the injury (mild, moderate, severe) (6). The most common injury among these is mild traumatic brain injury (mTBI), often called a concussion, commonly associated with symptoms of headache, dizziness, and confusion acutely following injury (7). Symptoms can also include decreased cognitive performance (forgetfulness, difficulty in learning), altered sleep habits, and altered emotional behavior, though symptoms tend to resolve within 7-10 days (8, 9). Long-term, mTBI has been linked to depression in up to 48% of patients one year following injury (10). Additionally, chronic traumatic encephalopathy (CTE), a recently discovered diseased characterized by cognitive deficiencies, volatile emotional behavior, and motor disease, has been linked to repeated traumatic brain injury (11). One hypothesized cause bridging the gap from mTBI to CTE are the formation of neurofibrillary tangles caused by the release of pro-inflammatory cytokines subsequently activating astrocytes and microglia upon mechanical stimulation (12). CTE is most commonly known from extensive

media coverage for affecting professional athletes that maintained a career in contact sports, specifically football; however, the military population suffering repeated blast injuries is an underreported yet significant demographic affected by traumatic brain injury (13).

Within the civilian population, young adults aged 15 to 24 years and the elderly over the age of 65 are at the greatest risk of suffering a TBI with the elderly having the highest mortality rates due to TBI (3). The most common cause of TBI occurs from falls, automobile accidents, or having the head strike or be struck by another object. Deployed military personnel are also at greater risks of suffering a TBI, specifically from blast injury, and are at greater risks of poor psychiatric health often suffering from post-traumatic stress disorder (14). The heterogeneity of TBI complicates creating an all-encompassing model for injury. It is necessary for models of TBI to simplify the insult itself to create a platform for replicable injury which can be used to study the cellular response to TBI (15). To this end, a fundamental study was performed to evaluate the responses of central nervous system cells to rapid decelerations coupled with biaxial stretching.

*Modeling Traumatic Brain Injury*

Expanding our knowledge on the manner physical stimulation is translated into a biological response will be of vital importance to understand, predict, and treat TBI. Attacking this issue can be quite difficult; one must understand the mechanical properties of brain tissue, the nature of the mechanical forces during TBI, and the mechanisms within the cell that sense and respond to these forces.

The tissue response of the brain to mechanical forces has been observed by performing mechanical testing on cortical tissue. The brain can be described as a viscoelastic material

possessing non-linear stress-strain behavior, hysteresis, and changing mechanical properties depending on strain rate (16). Understanding the mechanical properties of brain tissue can help produce accurate finite element models that can be used to predict pressures, stresses, and strain within the brain during TBI (17, 18). The nature of the mechanical stimulation can vary greatly as no single factor can predict the severity of injury (19). Factors can include rapid linear accelerations, rotational accelerations, the direction of impact, and impact duration (20). Linear accelerations have been shown to produce pressures, compression, and stretching which are one potential pathway to altered biological function. Likewise, rotational accelerations can produce shearing and stretching of cells inducing an injury response. A threshold level of an 18% stretch on neurons has been suggested to invoke traumatic axonal injury, though this was performed in an animal model and may not translate to the human injury tolerance level (21). The findings from studies investigating biomechanics of head injury creates parameters for *in vitro* and *in vivo* models to replicate.

Methods for modeling TBI *in vitro* and *in vivo* have been extensively reviewed (6, 22). Observing biological phenomena *in vitro* rarely translate directly to human physiology, therefore multitudes of animal models have been designed to study TBI in a complex system acting as an intermediate step. *In vivo* models for TBI reconstruct the mechanical stimulation of a traumatic brain injury. The most common TBI model used in animal studies is the fluid percussion injury. Briefly, this model produces TBI by way of a fluid pressure wave triggered by a weighted pendulum striking a lateral fluid column propagating the pressure wave onto an exposed surface of the brain resulting in cognitive and motor defects as well as biomarkers of injury (23). First reported by Dixon *et al.,* controlled cortical impact is another popular model for TBI utilizing a piston to strike exposed brain tissue at high rates creating a focal injury that is highly

reproducible (24, 25). Weight drop models require a substantial mass confined in a guide tube to be released from a height and strike the animal's head directly or on a plate covering the head causing diffuse injury (26, 27). Blast injury models inspired from soldiers exposed to explosions from the Iraqi and Afghan wars typically require placement of an animal into a metal tube that carries a pressure wave triggered by air or an explosion down the tube to the exposed animal (28). Finally, models using angular acceleration as the only means of mechanical stimulation by sudden twisting of the animal's head have been reported to cause diffuse brain injury (29). However, *in vivo* models suffer in isolating and observing specific biological phenomenon, controlling and measuring cellular and tissue mechanics, experiencing greater variability animal-to-animal, and requiring substantial increases in monetary cost for experiments.

*In vitro* TBI models are advantageous because of the ability to investigate specific pathobiological phenomena by tightly controlling experimental variables and mechanical stimulation. Commonly, *in vitro* models will utilize primary cultures, mixed cultures, or organotypic slice cultures (30). Primary cultures allow one to investigate specific pathways and mechanisms for one cell type while mixed cultures can provide insights into the interplay between different cells in mounting a response to injury. One common injury model requires the stretching of cell cultures or organotypic slice cultures on an elastic membrane (31). La Placa and Thibault developed a model invoking shear stress on neuronal cultures (32). Compression models have also been developed by dropping weights onto cell cultures (33). The wide plethora of *in vitro* TBI models examines specific mechanisms of injury providing specific insights into an injury response. To this end, we sought to develop an *in vitro* TBI bioreactor capable of applying multiple types of mechanical stimulation to primary cultures to increase the knowledge of the behavior of cells after suffering a traumatic brain injury.

*The Role of Astrocytes in the Central Nervous System*

The central nervous system (CNS) remains one of the most complex and least understood organ systems in the body. The CNS is comprised of the brain and spinal cord and acts as the integration center for receiving sensory information and transmitting a response to the rest of the body. Within the parenchyma of the brain and spinal cord, cells can be classified as either neuronal, endothelial, or glial cells. Neurons function by converting chemical, mechanical, or temperature stimuli into an electrical signal. The electrical signal known as an action potential is relayed to other neurons ultimately invoking a cognitive and motor response. Neurons are the functional cell type within the CNS responsible for our ability to sense our surroundings, form consciousness and thought, develop emotions, and generate signals for the body's organs to function. Endothelial cells create the vascularization within the brain playing a pivotal role of supplying CNS cells with nutrients and gas transport from the blood while blocking the passage of large molecules and pathogens. In approximately equal number to neurons is the "glue" of the brain in glial cells acting to support neuronal health, guide neurons in development, and regulate synapse formation (34). Glial cells include microglia, oligodendrocytes, and astrocytes. Microglia act as immune responders to pathogens entering the CNS as well as phagocytes to remove apoptotic cells. Oligodendrocytes are primarily found within the white matter of the CNS and are responsible for producing myelin sheath. Myelin created by oligodendrocytes act as an insulating barrier encircling axons to increase the speed of the action potential. Astrocytes carry out many essential functions including the production of extracellular matrix within CNS tissue and is the focus of this research henceforth.

Astrocytes are specialized glial cells responsible for maintaining homeostasis for neurons critical to survival (35). Astrocytes can be subdivided into two groups; protoplasmic astrocytes

are located in gray matter rich in neuronal cell bodies while fibrous astrocytes are found in the white matter where myelinated axons and oligodendrocytes are localized interacting with the nodes of Ranvier (36). However, the broad grouping of astrocytes into two groups may not be accurate as growing evidence supports heterogeneity of astrocytes in different regions of the brain. Astrocytes also bridge the gap between neurons and blood vessels modulating blood flow to specific regions of the brain by signaling endothelial cells to constrict or dilate controlling blood flow based on synaptic activity of the neighboring neurons (37). Astrocytes are also believed to aid in formation of the blood-brain barrier with end-feet coming into direct contact with endothelial cells (38).

At the synapse of neurons, astrocytes facilitate the recycling of neurotransmitters by uptaking released neurotransmitters and converting the molecules back to precursors that are then delivered to the axon terminal to be reused by the neuron (39). Though astrocytes do not 'fire' propagating an action potential like neurons, growing evidence indicates astrocytes participate in passing and modulating signals at the synapse. Known as the 'tripartite synapse', astrocytes possess G protein-coupled receptors that can be activated by neurotransmitters released from the presynaptic neuron like glutamate causing a rise in calcium levels within the astrocyte (40, 41). Evidence has shown in response to increased intracellular calcium astrocytes may release gliotransmitters such as glutamate, GABA, and ATP into the synapse (42). Studying the tripartite synapse is still in its infancy as many questions remain on the mechanisms involved in the release of gliotransmitters and if neurons truly respond to gliotransmitters.

Astrocytes are believed to tightly regulate interstitial fluid volume in the brain through the aquaporin-4 water channel (43). For energy, astrocytes act as the mediator of the uptake of glucose from the blood stream to neurons. Astrocytes also act to store glycogen that can be

metabolized and delivered to neurons as lactate during periods of hypoglycemia or localized high activity (44).

Additionally, astrocytes generate the ECM in the CNS. As in other tissues, the ECM acts to create structure and provide chemical cues to cells. In development, astrocytes can guide axons by secreting chondroitin sulfate proteoglycans (CSPGs) and tenascin-C that prevents axons from growing across these extracellular matrix proteins (45). The ECM of the CNS is unique in that it lacks the fibrous collagen backbone observed in other tissue's ECM and instead creates a mesh of glycoproteins and proteoglycans chiefly relying on hyaluronic acid. Surrounding blood vessels, astrocytes deposit a basement membrane comprising of laminin, fibronectin, heparin sulfate proteoglycans (HSPG), and collagen IV functioning to maintain the blood-brain barrier (46). Within the parenchyma, the most prominent ECM feature are perineuronal nets localized at synapses. Perineuronal nets are comprised of dense meshwork of CSPGs, tenascins, and hyaluronic acid and are believed to function to provide structure to the synapse and allow synaptic plasticity (47). Likewise, the neural interstitial matrix is built by the same proteoglycans as the perineuronal nets, though are located away from synapses. When exposed to insult or injury, astrocytes have the capacity to remodel the extracellular environment to minimize damage to surrounding tissue. It is less understood how astrocytes recognize injury and what ultimately triggers the remodeling of the ECM following injury.

*The Injury Response in the Central Nervous System*

Astrocytes are known to respond to any CNS insult like traumatic brain injury, formally known as reactive gliosis. *In vivo* and *in vitro* studies alike have demonstrated astrocytes proliferating at the site of injury, increase expression of intermediate filaments glial fibrillary acidic protein (GFAP) and vimentin, and increase expression of chondroitin sulfate

proteoglycans, laminin, and collagen IV (48-50). With TBI, one potential side effect is increased cranial pressure caused by edema in the brain. As mentioned previously, astrocytes tightly regulate the volume of interstitial fluid within the brain. Upon injury, research suggest astrocytes swell within hours causing an increase intracranial pressure with increased pressure correlating to poorer patient outcomes (51). Swelling has been suggested to be incited by increased expression of aquaporin-4 water channel as well as the activation of nuclear factor-κB (NF-κB) (52, 53).

Another known response to traumatic brain injury is the breakdown of the blood-brain barrier (BBB). Increased permeability of the BBB is an additional source of fluid build-up and greater intracranial pressure (51). Increased permeability of the BBB allows immunoglobulin G and albumin pass the BBB causing an inflammatory response in the parenchyma of the CNS (54). The initiation of an inflammatory response can create a signaling cascade causing the release of cytokines such as tumor necrosis factor-α and interlukin-1β that are toxic to neurons and cause reactive gliosis (54). Ultimately, the activation of astrocytes can lead to significant extracellular changes after injury.

Of particular interest to our group is understanding the extracellular changes driven by astrocytes which reshape the ECM after sustaining injury. In focal injuries (i.e. penetrating injuries, gunshot wounds), an evident scar region can form comprised of GFAP-positive astrocytes producing (CSPGs) in an effort to isolate the injury, thereby limiting the spread of inflammation and tissue damage. In the short term, this is advantageous for limiting damage to neighboring healthy tissue; however, the scarred region inhibits long-term neuron growth, thus preventing the reformation of any neural connections lost during injury. Astrocytes further modify the extracellular environment with increased expression of fibronectin and laminin

believed to aid in macrophages clearing dying cells and repair the BBB, respectively (55). However, in diffuse traumatic brain injury, an injury site and glial scar formation may not be apparent. A greater understanding of changes in the extracellular environment driven by astrocytes could provide needed insights into the diagnosis and treatment of TBI. Further, it is our goal to determine the mechanical mechanisms in which astrocytes sense injury and how astrocytes may affect the extracellular environment.

*Thesis Statement*

Previously, we have reported a novel bioreactor capable of delivering mechanical stimulation mimicking a traumatic brain injury (56). The bioreactor is unique in that it implements inertial loads onto cells while simultaneously applying biaxial strain. We hypothesize mechanical stimulation causes fundamental changes in the composition and production of extracellular matrix proteins by astrocytes at acute time points after a TBI event. The aims for this project were to first validate the bioreactor mimicked mechanical stimulation experienced by the brain that results in a traumatic brain injury. Validation of the injury model was accomplished by observing astrocyte survival and behavior for key markers of reactivity. Extracellular matrix alterations were observed in astrocyte cultures through monitoring gene expression, cytokine secretion, and immunofluorescence labeling of structural and adhesion proteins. The outcome for this study was to observe and present astrocyte behavior and alterations to the extracellular environment after simultaneous exposure to inertial loads and stretch analogous to a TBI, while investigating potential cumulative effects with multiple injuries, and observe changes to the astroglial response to injury when cultured with or without serum.

## II. Material and Methods

*TBI Bioreactor Fabrication*

The TBI bioreactor used is that which was previously reported by Heller *et al*. and can be used for an in depth characterization of the bioreactor (56). The TBI bioreactor contains four components; a guide rod, drop shuttle, polypropylene cell culture drum and a spring-damped base. The guide rod is comprised of a steel rod (diameter = 3cm, length 2m) press-fit into an aluminum base plate (Fig 1A). The guide rod acts to constrict the motion of the drop shuttle to one vertical direction. The shuttle is made from two aluminum plates encompassing an intermediate polypropylene plate (Fig 1B). The top aluminum plate has a linear bearing attached to allow nearly frictionless motion along the guide rod. Six small circular holes were cut from the polypropylene layer that act to house the cell culture drums during impacts. The bottom aluminum plate contains six circular holes coincident to the openings in the polypropylene layer that allow custom indenters to apply biaxial strain to the culture upon impact (Fig 1C). Increasing the height of the indenter coincides with increased strain on the cell culture. Indenter heights of 5mm caused 20% biaxial strain on the cell culture. Cell culture drums utilize a porous polyurethane foam created using a technique familiar to our lab (Fig 2). Wetted sugar was packed into silicone molds and dried in an oven at 70ºC for 30 minutes. Polyurethane dissolved in dimethylacetamide (DMAC) (10% weight by volume) was pipetted drop by drop onto the sugar mold. Polyurethane was cured and sugar dissolved by placing molds in repeated deionized water baths over three days. Medical grade polydimethylsiloxane (PDMS) placed beneath the scaffold is secured by a silicone O-ring and creates a watertight seal. The impact base is comprised of a square steel plate mounted onto an interchangeable spring (Fig 2).

*Characterization of TBI Bioreactor*

A uniaxial ±300G accelerometer was mounted onto the drop shuttle and connected to a 16-bit data acquisition card (National Instruments). Samples were collected at 10,000 Hz. A custom-built LabVIEW program converted accelerometer voltage output (-2.5V to 2.5V) to gravitation. The bioreactor was characterized with three different spring bases for impact duration (n=25) and peak deceleration. A linear relationship for the peak deceleration for each spring was established by releasing the drop shuttle at 25cm increments up to 175cm above the spring-damped base (n=5, per height). Biaxial strain was validated optically using a digital camera and three microspheres as markers. Pre-stretch and post-stretch images were acquired. Monitoring the change in distance between each microsphere after deformation generated values for circumferential, radial, and shear strain.

*Isolation of primary rat astrocytes*

Primary cortical rat astrocytes were isolated from 1-day old neonatal rat pups following a modified procedure previously reported (57). Rat astrocyte cortexes were separated from all meninges and blood vessels and digested in dissociation media (0.2% collagenase/DNase) for two hours. Dissociated cells were treated with 0.25% Trypsin (Gibson), then passed through a cell strainer. Finally, cells were rinsed and centrifuged in 1X PBS supplemented with glucose. Mixed glial and neural cells were seeded onto laminin-coated cell culture flasks. Mixed glial cultures were grown in DMEM F-12 media (Gibco) supplemented with 10% Fetal bovine serum (FBS), 1% Penicillin/Streptomycin, and 1% l-Glutamine and allowed to reach confluency (7-9 days) with media exchanges occurring every two days. Mixed glial cultures were then subject to orbital shaking for twenty-four hours at 200 RPM to detach loosely adherent neurons, microglia, and oligodendrocytes. Purified astrocytes were passaged to culture flasks until the desired cell

number was achieved. Astrocyte purification was validated by immunostaining for the presence of glial fibrillary acidic protein (GFAP), a common marker for astrocytes (Appendix A) (58, 59). A threshold of 90% GFAP positive cells was used in determining if cultures were astroglial enriched cultures or mixed glial cultures (60). Cultures were maintained in an incubator at 37°C, 95% humidity, and 5% $CO_2$.

*Experimental Design*

Astrocyte cultures were divided into multiple subsets to explore potential differences in cellular response given different culturing parameters. The first parameter explored was the effect of serum-containing media (10% fetal bovine serum) against serum-free media (N-2 Supplement) (61, 62). The difference in media aimed to mimic an open head injury with the presence of blood at the injury site against a closed head injury where blood may not be present throughout the injury. The second parameter compared the reaction of cells to a single TBI mimetic impact against those receiving a second TBI mimetic impact twenty-four hours after the first impact. Previous work has shown graded cognitive differences and astroglial reactivity indicative of a cumulative response to TBI as well as heightened sensitivity to injury shortly after an initial impact (26, 63, 64). The third parameter evaluated the response of astrocyte cultures to receiving a 150G impact with 20% biaxial strain against cultures receiving a 150G impact without strain. To this end, we sought to compare the nature of the stimulus that brought about reactivity and changes in astrocyte behavior post injury. A total of 8 experimental groups were tested represented by all combinations of the parameters listed previously (n=4 minimum per group).

*Mimetic TBI Impacts*

Prior to seeding, cell culture drums were incubated in laminin (10ug $mL^{-1}$, Gibco) overnight to promote cell adhesion. Astrocytes were seeded onto the center (10mm diameter) of the fabricated TBI bioreactor drums at a concentration of $4.5\times10^5$ cells per drum. Cells were given seventy-two hours to adhere and proliferate within the drum. Forty-eight hours prior to the first impact, cultures designated as serum-free were switched to serum-free media. Neurobasal serum-free media comprised of DMEM/F-12 media with 1% N-2 Supplement (Gibco), 1% Pen/Strep, and 1% l-Glutamine. Releasing the drop shuttle 170cm above the base corresponded to a 150G impact. The use of 5mm indenters onto the base of each cell culture provided 20% biaxial strain. Medium was removed from each cell culture immediately before impact and fresh medium added immediately following impact. The time out of media was recorded for each culture, spending a total of 5-7 minutes out of media. A second impact was given twenty-four hours after the initial impact to cultures designated for that parameter.

*Cell Viability Assay*

Relative cell viability was established using a modified MTT cell proliferation procedure (Life Technologies). Cultures received mimetic TBI impacts as described above. Forty-eight hours following impact, cultures were rinsed with DMEM/F-12 media without phenol red and incubated in 1mL MTT solution (1.2mM) for two hours. 75% of the solution was aspirated following incubation and replaced with dimethyl sulfoxide (DMSO). The resulting precipitate was solubilized by agitation through repeated pipetting. Solution was transferred to a 96 well plate and absorbance at 540nm was measured (BioTek Synergy Mx). A standard curve was generated using known cell culture concentrations and experimental results were referenced to

the standard. Reported cell viability is expressed relative to the single impact, serum-containing control.

*Reverse transcription-PCR (RT-PCR) analysis*

Two separate RT-PCR experiments were performed targeting reactive gliosis and extracellular matrix substrates. Exploring reactive gliosis, extraction of cells from culture for all experimental groups (n=4-5/group) occurred twenty-four hours following the terminal impact while for extracellular matrix production extraction occurred six hours following the final impact for all experimental groups (n=4/group). Cell culture foams were removed from the cell culture drum using a scalpel and stored in RNAProtect (Qiagen) at -80°C. RNA was isolated using RNeasy Mini Kit Plus (Qiagen) following manufacturer's protocol. Genomic DNA was eliminated by passing RNA through gDNA Eliminator Spin Column (Qiagen) during the RNA isolation procedure. RNA samples were reverse transcribed using iScript cDNA Synthesis kit (Bio-Rad) following the manufacturer's protocol. cDNA samples were appropriately diluted for RT-PCR analysis so that all samples contained the same concentrations of cDNA. In studying reactive gliosis, GFAP, S100B, and Vimentin primers were commercially purchased (Bio-Rad). For extracellular matrix production, primers for Collagen I, Versican, and Neurocan were also commercially obtained (Bio-Rad). SsoAdvanced Universal Sybr Green Supermix (Bio-Rad) acted as the fluorescent label to monitor amplification of the target genes. ECM protein expression was normalized to GAPDH expression relative to the control sample using the $\Delta\Delta C_t$ method. Cycling conditions were 40 cycles at 95°C for 5 seconds and 60° for 30 seconds following manufacturer's recommendations (Bio-Rad CFX96 Touch).

*Extracellular and Inflammatory cytokine analysis*

Cell culture supernatants were collected forty-eight hours following the final impact. Cytokine concentrations from cell culture supernatants were measured using colorimetric sandwich ELISAs (R&D Systems) for Matrix Metalloproteinase 2 (MMP-2), Tissue Inhibitor of Metalloproteinases 1 (TIMP-1), and Transforming Growth Factor Beta 1 (TGFβ-1) following the manufacturer's protocol. Cytokine concentrations are presented relative to viable cells found from the MTT assay and reported as production of cytokine per cell (fg $cell^{-1}$)

*Measurement of Matrix Accumulation*

To investigate the effect of repeated impact on cellular matrix accumulation, astrocyte-seeded porous polyurethane foam culture inserts were impacted (150g combined with 20% strain) every 2-3 days for a total of three weeks (9 impacts total). The repeated impact regime was designed to imitate an in-season football training schedule, during which athletes have been shown to experience up to 900 head impacts. Serum-containing media (10% FBS) was exchanged every 2-3 days throughout the conditioning period. Following the three-week conditioning period, impacted and static control samples were fixed in 4% paraformaldehyde, permeabilized with 0.05% triton and stained for the presence of collagen type I (Sigma 1:500) laminin, (Sigma 1:1000) and chondroitin sulfate proteoglycan (CSPG, Sigma 1:500) followed by the appropriate fluorescently labeled secondary detection antibodies (Life Technologies, Alexafluor, 1:500). The intensity of fluorescence against collagen, laminin, and CSPG for each sample was used to estimate matrix accumulation. Immunoreactivity was quantified using relative fluorescence intensity for each scaffold measured with the aid of a plate reader (Synergy HT, Bio-Tek Instrument Inc., VT) using techniques familiar to our group. Cells were counterstained with the nuclear labeling reagent DAPI. Fluorescence values were normalized to

cell count for each sample. Cell counts were estimated from DAPI images. Microscopic images were also obtained for qualitative analysis and comparison.

*Statistics*

Results are presented as mean ± SEM. A two-way ANOVA with post hoc Tukey test determined statistical difference for experimental groups in cell viability assay, cytokine assay, and immunostaining. Student's T-test was used to determine statistical differences for gene expression and characterizing the device. P values less than 0.05 indicate significantly different populations.

## III. Results

*Device Characterization*

The first aim was to investigate the critical release height so that the entire shuttle was subject to linear decelerations and impact durations analogous to that felt during a TBI event. Impact duration followed an expected trend with the stiff spring (spring constant, 959lbs $in^{-1}$) having the shortest impact duration and the flexible spring (90lbs $in^{-1}$) experiencing the longest impacts (Table 1). The desired impact durations matching reported physiological conditions were met using the medium (312lbs $in^{-1}$) or flexible spring giving impact durations of 9.2 ± 1.2ms and 19.3 ± 0.5ms respectively compared to 1.6 ± 0.3ms for the stiff spring(65). Impact duration was not affected by the drop height of the shuttle for each spring. Each spring-damped base is significantly different from the others for impact duration. For each spring, a linear relationship between peak deceleration and release height exists (Table 1). The flexible spring base reached a maximum deceleration of 59.1 ± 4.3G when dropped from the highest release point. Though some reports have described individuals with concussive symptoms after experiencing similar head decelerations, it does not encompass all individuals who may have a higher threshold to TBI events. In comparison to the flexible spring, the medium and stiff spring reached maximum decelerations of 158.2 ± 28.8G and 184.5 ± 26.6G when dropped from the highest release point. Measured impacts reaching these extreme decelerations are likely to cause symptoms associated with mild or severe TBI(66). From these characterization trials, we chose to use the medium spring-damped base. Using the established linear relationship, for all experiments 150G impacts were obtained by dropping the shuttle from 170cm above the medium spring-damped base.

*Cell Viability*

A modified MTT assay was used to quantify cell survival for the experimental group relative to control groups (Fig 3). Cultures receiving serum and a single impact exhibited the strongest cell survival, retaining 79.4 ± 6.6% viable cells following a mimetic TBI compared to the single impact, serum-containing control. Withholding serum from media contributed to a trend of decreased cell survival as the control and single impacted cultures viable cell counts were 81.9 ± 11.4% and 81.9 ± 12.1% respectively relative to the serum control. Furthermore, a second impact significantly decreased viable cell counts to 59.0 ± 4.5% in impacted cultures supplemented with FBS and 45.4 ± 11.3% in serum-free cultures relative to the control. The combination of serum-free media and two impacts created a particularly hostile environment for astrocyte survival. Subsequent long-term studies were consistent with these findings as cultures withheld from serum were not capable of surviving multiple impacts over a 3-week span (data not shown).

*Gene Expression for Astrocyte Reactivity*

We hypothesized astrocytes would increase expression of intermediate filaments GFAP and vimentin as well as a reported inflammatory marker S100B based on previous *in vivo* and *in vitro* studies(67, 68). Surprisingly, we did not observe an increase in any of these proteins 24 hours after mimetic TBI impacts (Fig 4). Across all conditions, impacted cultures decreased GFAP and S100B compared to all controls ($p<0.0001$). The number of impacts or media type did not have an effect on gene expression. Vimentin expression remained relatively unchanged compared to controls with the exception of astrocytes receiving serum-containing media and impacted once decreasing relative gene expression compared to control ($p=0.0005$). Although astrocytes withheld from serum receiving a single mimetic TBI upregulated vimentin three-fold,

this result was not significant from the control (p=0.071). GFAP expression was decreased across all experimental groups, though only significantly in one impact serum groups (p=0.0011) and astrocytes withheld from serum receiving two mimetic TBI's (p=0.0238). S100B was consistently downregulated by all astrocytes receiving mimetic TBI with cultures receiving two impacts while withheld from serum displaying the greatest decrease from the control.

*Extracellular Matrix Gene Expression*

Quantitative reverse transcriptase PCR analysis for structural ECM proteins (Fig 5) revealed that astrocyte cultures receiving two mimetic TBIs exhibited decreased collagen I expression ($p<0.0001$, serum and serum-free). The absence of this observation in the single TBI condition could indicate a cumulative effect of TBI. Likewise, vesicant (p=0.0040) and neurocan expression (p=0.0039) decreased for astrocytes impacted twice receiving serum-containing media. Versican expression was also decreased in the single impact serum-containing media condition (p=0.0136), indicating a combination of impacts and presence of serum could suppress versican expression. Neurocan expression levels for all impacted groups decreased compared to controls, though only significantly as discussed previously. Overall, cultures receiving serum-containing media and two impacts exhibited reduced expression for ECM proteins, indicating that astrocytes were producing extracellular matrix at a dampened rate compared to healthy astrocytes.

*Cytokine Secretion*

Secreted cytokines regulating ECM turnover and inflammatory cytokines promoting ECM production were normalized to the viable cells found previously and reported as the production of cytokine (fg) per astrocyte (Fig 6). Production of TGFB-1 was affected by the

presence of serum and the number of impacts. Cultures receiving serum-containing media demonstrated an increased expression of TGFB-1 compared to serum-free cultures. Interestingly, astrocytes in serum-free media receiving a second impact increased TGFB production ($5.9 \pm 0.5$ fg cell$^{-1}$) compared to controls ($2.8 \pm 0.8$ fg cell$^{-1}$), an expected trend that was not evident in any other experimental group. A common trend was observed in astrocytes receiving mimetic TBI decreasing MMP-2 production no matter the media type or number of impacts. Excluding cultures in serum-free media receiving two impacts, all other impact conditions decreased MMP-2 by at least half compared to the controls. A significant difference was not observed in MMP-2 production across number of impacts, but was observed in media type. One of the inhibitors for MMP-2, TIMP-1, was not affected by injury, number of impacts, or media type. A miniscule trend of increased TIMP-1 production was observed for most injury conditions; however, it was not considered a significant increase. Interestingly, TIMP-1 production dominates MMP-2 production in both control and injured astrocytes. TIMP-1 inhibits MMP-2 in a 1:1 stoichiometric ratio, therefore we quantified the overall inhibitory behavior of degrading ECM in astrocytes after impacts by investigating the ratio of TIMP-1 to MMP-2 produced by astrocytes. Comparing across media types, cultures receiving serum supplemented media had a significantly increased TIMP-1/MMP-2 ratio. Within one or two impact groups there were no statistical differences. In all cohorts, astrocytes impacted with strain experienced a significant increase in TIMP-1/MMP-2 ratio. This indicates that the combination of serum-containing media (hemorrhaging) and mechanical stimulation from stretching and impacts can create an inhibitory environment for the degradation of ECM molecules. An important outcome of note is the inhibited release of important growth factors bound into the ECM. This could play

into the somewhat delayed activation of astrocytes after injury as some reports have shown astrocyte reactivity peaking 4-7 days following injury(69).

*Matrix Immunostaining*

Using immunostaining, collagen, laminin and CSPG accumulation as well as astrocyte distribution were evaluated following three weeks of conditioning for both impacted and control porous polyurethane samples. At the end of the three-week conditioning period, astrocytes were well-distributed throughout the scaffold for both control and impacted cultures. Quantitative immuno-histochemical analysis demonstrated that the relative intensities of immunoreactivity to CSPG, laminin and collagen type I were decreased when compared to un-impacted controls ($p < 0.05$) Qualitative observations confirmed the quantitative analysis (Fig. 7).

## IV. Discussion

We present a unique bioreactor subjecting cells to mechanical stimuli that would likely lead to traumatic brain injury *in vivo*. The bioreactor provides a model between pure *in vitro* and *in vivo* studies. This bioreactor, to our knowledge, is unique in its ability to simultaneously expose cells to rapid decelerations, like that in an impact resulting in TBI, while applying biaxial strain. Moreover, three-dimensional cultures are an important parameter to better mimic the structure of native tissue capturing cell pathology that may be lost when cultured in 2D (70). The created bioreactor is advantageous because of the flexibility in experimentation. In this study, we examined astrocytes cultured in three-dimensional foams; however, the foam can be interchanged allowing for the study of cells in monolayer, three-dimensional hydrogels or even organotypic cultures. The bioreactor also has the ability to house primary cells, co-cultures of astrocytes and neurons, or mixed glial cells. With the complex nature of the bioreactor, the mechanical stimulation given to individual cells is less understood. The pore structure of each foam used for cell culture is unique making it impractical to attempt to map stresses and strains across the entire foam. Additionally, the bioreactor cannot impose angular decelerations often associated with TBI, nor control strain rate. Both *in vivo* and *in vitro* studies alike have demonstrated a graded injury response to rotational accelerations and strain rates (71, 72). Our results support astrocyte cultures respond to the mechanical stimulation delivered by the bioreactor.

Several *in vitro* models utilize a stretch injury, while neglecting inertial loading on the cells. Some may argue astrocytes in our bioreactor are incapable of sensing inertial forces because of the small mass of individual cells (~$3x10^{-9}$ g) resulting in minute forces on the cell. Other cell types have exhibited sensitivity to inertial forces. Lung, cardiac, chondrocyte, and

osteoblasts can modulate ECM production triggered by changes in gravitational forces (73-76). Applying vibration to mouse vertebrate *ex vivo* and *in vivo* stimulated production of extracellular proteins (77). An *in vitro* model inducing shear strain on organotypic cultures using inertial loading increased cell death after injury (78). Because of the sensitivity to Newtonian forces exhibited in other cell types, it is reasonable to assume astrocytes are capable of sensing and responding to the decelerations created by our bioreactor modulating the ECM. Under the experimental regime described above, astrocytes experiencing a 150G deceleration without biaxial strain altered expression and production of ECM proteins often exhibiting a medial expression between control and 150G impacts with strain (Supplemental Figure 1).

A hallmark of injury to the central nervous system is reactive astrogliosis, resulting in the proliferation of astrocytes, increased expression of intermediate filaments after injury, and increased production of CSPGs (65, 66). We observed forty-eight hours following injury, the number of viable cells was decreased between 13-55% depending on the media type or impact number. These values are similar to a stretch injury TBI model performed *in vitro* (79). We also report astrocytes decreased GFAP expression after experiencing injury in our model. Zhao *et al*. observed decreased immunoreactivity to GFAP in hippocampal astrocytes at acute time points after TBI in a rat model as well as pronounced astroglial death (80). This could indicate the injury applied in our model is severe, leaving astrocytes in a damaged state. In comparison, though not explicitly stated, examination of human cerebellum after TBI displayed correlations between decreased GFAP expression and increased caspase 3 expression, indicative of cell apoptosis (81). The decreased expression of S100B can support the claim that astrocytes are severely damaged in our model as S100B has shown protective effects in neuronal-glial co-cultures *in vitro* after stretch injury (68). Subsequently, high incidences of neuronal death have

been observed in the same brain regions of astroglial death, which may contribute to the symptoms associated with TBI (80). An interesting parallel is the decrease in GFAP expression in astrocytes by depressed and suicidal patients (82, 83). Long term depression and fatigue have been associated with TBI (84). Although we do not prove that inertial impacts induce these long term symptoms, it is an observation of note to see similar effects in our experiment.

We observed differences in astrocyte behavior in response to a single injury, two injuries, and multiple injuries. With respect to ECM expression, a second injury caused significant decreases in collagen, versican, and neurocan expression in the serum-containing cohort. After implementing multiple injuries over a three-week time period, we observed decreased ECM accumulation in injured cultures. These observations suggest the number of impacts may have a role in how astrocytes modulate the ECM. Multiple impacts have proven translational from *in vitro* models to clinical studies. It is widely accepted that individuals with a previous history of TBI are more susceptible to a second injury, especially in the days following a TBI (85). In an *in vitro* stretch injury model, co-cultures of neuronal and glial cells exhibited increased uptake of propidium iodide after a second injury indicative of cell damage, thus demonstrating how CNS cells are sensitive to a second injury (86). Likewise, repeated fluid percussion injury subjecting Long-Evans hooded rats to single or multiple injuries demonstrated behavioral differences, memory impairment, and increased inflammation short-term and long-term (87). To our knowledge, this is the first study to investigate the potential cumulative effect of repeated TBI on the composition and production of extracellular matrix.

The extracellular matrix in the brain is unique in that it is constituted by glycoproteins (and proteoglycans as opposed to other ECM in tissues having a fibrillary base, typically collagen. ECM in the brain functions to provide structure to CNS cells, guide axon growth in

development, form perineuronal nets, and create the blood brain barrier. We examined the potential fibrotic-like scar formation through the expression of collagen I. Although lacking fibrillar elements in the central nervous system, astrocytes have been reported to produce fibrillary collagen *in vitro* (88). Fibrotic scars have been reported in lesion injuries to CNS, though this is likely induced by invading meningeal fibroblasts (89). In our study, we found a suppression in expression of collagen I in cultures receiving multiple injuries. It has been shown that TGFB-1 increases the production of collagen in astrocyte (89), thus the static nature of TGFB concentrations between control and TBI groups coupled with the downregulation of collagen indicates a strong inhibitory pathway is likely in play. Epidermal growth factor, tumor necrosis factor alpha, and interferon gamma all suppress the production of collagen in astrocytes *in vitro*(88). Surprisingly, we did not observe indications of the formation of a glial scar or increased matrix metalloproteinase activity. This observation is not without precedent, as versican, neurocan, aggrecan, and phosphacan have been reported to decrease expression near the injury site of a controlled cortical impact in a rat model (90). It appears clear that the injury invoked on astrocytes in this model do not initiate the formation of a glial scar. The decreased extracellular matrix protein expression coupled with suppressed production of MMP-2 indicates the injured astrocytes are incapable of turning over damaged ECM, while also unable to produce new ECM. In studies inhibiting MMP-1, synaptogenesis after injury was hampered with MMP-1 inhibited, thus suggesting degenerating ECM after injury is crucial for proper recovery (91). The suppressed production of MMP-2 could correlate to decreased brain plasticity after TBI. The negative affects of damaged ECM on cells has been demonstrated in mesenchymal stem cells when implanted into decellularized scaffolds isolated from cardiac tissue after infraction (92).

Serum-containing media simulates a disruption of the blood brain barrier after injury, often scene in moderate to severe cases of TBI. The serum-free condition with the high mechanical load presents a unique model in that astrocytes experience a severe TBI, yet are not exposed to the factors that would normally be released upon the disruption of the BBB found with severe TBI. While serum-containing conditions may be more physiologically relevant, withholding serum from cultures provides insights to the potential protective effects of the breakdown of blood vessels and subsequent release of blood upon injury. Serum-free conditions inherently reduce cell viability, as observed in both TBI and control serum-free conditions; however, impacting cultures resulted in a far greater reduction in viable cell counts. Comparatively, as little as 20% cell survival has been reported in astrocytes when deprived of serum (93). Long-term studies with serum-free cultures confirmed this as cells were incapable of surviving the impact regiment out to three weeks (data not shown). For ECM expression levels, we observed increased sensitivity in astrocytes cultured in serum-containing media. One possible explanation stems from decreased quantities of focal adhesions when astrocytes are deprived of serum, thus decreasing sensitivity to mechanical stimulation (94).

Overall, we present astrocytes modulate extracellular matrix in response to mechanical forces. We would be remised to not mention shortcomings in the experimental design. As stated previously, strain rate and angular accelerations are important parameters that effect the severity of injury. Unfortunately, with the present design of our device, we are incapable of controlling strain rate or applying angular accelerations. Further, we did not observe astrocyte behavior after mild TBI that complemented previous literature, instead likely applying an injury that initiated cell death and left surviving astrocytes in a severely damaged state. It would be of consequence to obtain a dose response curve to varying impacts by decreasing the release height of the shuttle.

We explored astrocytes response at acute time points; however, increasing the time in culture after injury may reveal alterations in ECM expression indicating the formation of a glial scar or simply resolving any alterations. A next generation TBI bioreactor is currently being created that will create a compression injury using a weight dropped onto astrocytes cultured in a hydrogel that mimics the brain's mechanical properties (Appendix B Figure 1). The impact has been characterized for the bioreactor and peak pressures can be estimated from this characterization (Appendix B Figure 2). The affect of other cell types on astrocytes after injury is not explored here but could alter the response to injury. To complement this work, understanding the mechanism in which astrocytes sense and respond to mechanical stimulation is a logical next step. Increased permeability to calcium is a response to mechanical stimulation in astrocytes, thus a reasonable target to investigate is a calcium-specific mechanotransducer (95). Influx of calcium is reported to initiate astrogliosis in the central nervous system, therefore investigating mechanosensitive calcium channels may increase the understanding of the mechanisms that are responsible for altering cellular behavior after TBI and may reveal a therapeutic target for treating injury (96). Preliminary work has begun to investigate the potential role of calcium permeable channel transient receptor potential cation channel subfamily vanilloid member 4 (TRPV4). As a preliminary step for future research, the influx of calcium has been observed by astrocytes in response to a TRPV4 agonist (Appendix C Figure 1).

## V. References


1. Menon DK, Schwab K, Wright DW, Maas AI, Int Interagency Initiative C. Position Statement: Definition of Traumatic Brain Injury. Archives of Physical Medicine and Rehabilitation. 2010;91(11):1637-40.

2. Langlois JA, Rutland-Brown W, Wald MM. The epidemiology and impact of traumatic brain injury - A brief overview. Journal of Head Trauma Rehabilitation. 2006;21(5):375-8.

3. Coronado V, Xu L, Basavaraju S, McGuire L, Wald M, Faul M, et al. Surveillance for traumatic brain injury-related deaths--United States, 1997-2007. MMWR Surveillance Summaries. 2011;60(SS05):1-32.

4. Marin JR, Weaver MD, Yealy DM, Mannix RC. Trends in Visits for Traumatic Brain Injury to Emergency Departments in the United States. Jama-Journal of the American Medical Association. 2014;311(18):1917-9.

5. Ma VY, Chan L, Carruthers KJ. Incidence, Prevalence, Costs, and Impact on Disability of Common Conditions Requiring Rehabilitation in the United States: Stroke, Spinal Cord Injury, Traumatic Brain Injury, Multiple Sclerosis, Osteoarthritis, Rheumatoid Arthritis, Limb Loss, and Back Pain. Archives of Physical Medicine and Rehabilitation. 2014;95(5):986-95.

6. Morrison B, Elkin BS, Dolle JP, Yarmush ML. In Vitro Models of Traumatic Brain Injury. In: Yarmush ML, Duncan JS, Gray ML, editors. Annual Review of Biomedical Engineering, Vol 13. Annual Review of Biomedical Engineering. 13. Palo Alto: Annual Reviews; 2011. p. 91-126.

7. Scorza KA, Raleigh MF, O'Connor FG. Current Concepts in Concussion: Evaluation and Management. American Family Physician. 2012;85(2):123-32.

8. Hall RCW, Chapman MJ. Definition, diagnosis, and forensic implications of postconcussional syndrome. Psychosomatics. 2005;46(3):195-202.

9. Ling H, Hardy J, Zetterberg H. Neurological consequences of traumatic brain injuries in sports. Molecular and Cellular Neuroscience. 2015;66:114-22.

10. Hart T, Brenner L, Clark AN, Bogner JA, Novack TA, Chervoneva I, et al. Major and Minor Depression After Traumatic Brain Injury. Archives of Physical Medicine and Rehabilitation. 2011;92(8):1211-9.

11. Stern RA, Daneshvar DH, Baugh CM, Seichepine DR, Montenigro PH, Riley DO, et al. Clinical presentation of chronic traumatic encephalopathy. Neurology. 2013;81(13):1122-9.

12. Lucke-Wold BP, Turner RC, Logsdon AF, Bailes JE, Huber JD, Rosen CL. Linking Traumatic Brain Injury to Chronic Traumatic Encephalopathy: Identification of Potential Mechanisms Leading to Neurofibrillary Tangle Development. Journal of Neurotrauma. 2014;31(13):1129-38.

13. Goldstein LE, Fisher AM, Tagge CA, Zhang XL, Velisek L, Sullivan JA, et al. Chronic Traumatic Encephalopathy in Blast-Exposed Military Veterans and a Blast Neurotrauma Mouse Model. Science Translational Medicine. 2012;4(134):16.

14. Hoge CW, McGurk D, Thomas JL, Cox AL, Engel CC, Castro CA. Mild traumatic brain injury in US Soldiers returning from Iraq. New England Journal of Medicine. 2008;358(5):453-63.

15. LaPlaca MC, Simon CM, Prado GR, Cullen DK. CNS injury biomechanics and experimental models. Neurotrauma: New Insights into Pathology and Treatment. 2007;161:13-26.

16. Prevost TP, Balakrishnan A, Suresh S, Socrate S. Biomechanics of brain tissue. Acta Biomaterialia. 2011;7(1):83-95.

17. Shafieian M, Darvish KK, Stone JR. Changes to the viscoelastic properties of brain tissue after traumatic axonal injury. Journal of Biomechanics. 2009;42(13):2136-42.

18. Lamy M, Baumgartner D, Yoganandan N, Stemper BD, Willinger R. Experimentally validated three-dimensional finite element model of the rat for mild traumatic brain injury. Medical & Biological Engineering & Computing. 2013;51(3):353-65.

19. McCaffrey MA, Mihalik JP, Crowell DH, Shields EW, Guskiewicz KM. Measurement of head impacts in collegiate football players: Clinical measures of concussion after high- and low-magnitude impacts. Neurosurgery. 2007;61(6):1236-43.

20. Post A, Hoshizaki TB, Gilchrist MD, Brien S, Cusimano MD, Marshall S. The influence of acceleration loading curve characteristics on traumatic brain injury. Journal of Biomechanics. 2014;47(5):1074-81.

21. Bain AC, Meaney DF. Tissue-level thresholds for axonal damage in an experimental model of central nervous system white matter injury. Journal of Biomechanical Engineering-Transactions of the Asme. 2000;122(6):615-22.

22. Levin HS, Robertson CS. Mild Traumatic Brain Injury in Translation. Journal of Neurotrauma. 2013;30(8):610-7.

23. Alder J, Fujioka W, Lifshitz J, Crockett DP, Thakker-Varia S. Lateral Fluid Percussion: Model of Traumatic Brain Injury in Mice. Jove-Journal of Visualized Experiments. 2011(54):7.

24. Dixon CE, Clifton GL, Lighthall JW, Yaghmai AA, Hayes RL. A CONTROLLED CORTICAL IMPACT MODEL OF TRAUMATIC BRAIN INJURY IN THE RAT. Journal of Neuroscience Methods. 1991;39(3):253-62.

25. Chen YC, Mao HJ, Yang KH, Abel T, Meaney DF. A modified controlled cortical impact technique to model mild traumatic brain injury mechanics in mice. Frontiers in Neurology. 2014;5:14.

26. Kane MJ, Angoa-Perez M, Briggs DI, Viano DC, Kreipke CW, Kuhn DM. A mouse model of human repetitive mild traumatic brain injury. Journal of Neuroscience Methods. 2012;203(1):41-9.

27. Marmarou A, Foda MAA, Vandenbrink W, Campbell J, Kita H, Demetriadou K. A NEW MODEL OF DIFFUSE BRAIN INJURY IN RATS .1. PATHOPHYSIOLOGY AND BIOMECHANICS. Journal of Neurosurgery. 1994;80(2):291-300.

28. Long JB, Bentley TL, Wessner KA, Cerone C, Sweeney S, Bauman RA. Blast Overpressure in Rats: Recreating a Battlefield Injury in the Laboratory. Journal of Neurotrauma. 2009;26(6):827-40.

29. Fijalkowski RJ, Stemper BD, Pintar FA, Yoganandan N, Crowe MJ, Gennarelli TA. New rat model for diffuse brain injury using coronal plane angular acceleration. Journal of Neurotrauma. 2007;24(8):1387-98.

30. Kumaria A, Tolias CM. In vitro models of neurotrauma. British Journal of Neurosurgery. 2008;22(2):200-6.

31. Morrison B, Cater HL, Benham CD, Sundstrom LE. An in vitro model of traumatic brain injury utilising two-dimensional stretch of organotypic hippocampal slice cultures. Journal of Neuroscience Methods. 2006;150(2):192-201.

32. LaPlaca MC, Thibault LE. An in vitro traumatic injury model to examine the response of neurons to a hydrodynamically-induced deformation. Annals of Biomedical Engineering. 1997;25(4):665-77.

33. Sieg F, Wahle P, Pape HC. Cellular reactivity to mechanical axonal injury in an organotypic in vitro model of neurotrauma. Journal of Neurotrauma. 1999;16(12):1197-213.

34. Herculano-Houzel S. The Glia/Neuron Ratio: How it Varies Uniformly Across Brain Structures and Species and What that Means for Brain Physiology and Evolution. Glia. 2014;62(9):1377-91.

35. Cui W, Allen ND, Skynner M, Gusterson B, Clark AJ. Inducible ablation of astrocytes shows that these cells are required for neuronal survival in the adult brain. Glia. 2001;34(4):272-82.

36. Sofroniew MV, Vinters HV. Astrocytes: biology and pathology. Acta Neuropathologica. 2010;119(1):7-35.

37. Tran CHT, Gordon GR. Acute two-photon imaging of the neurovascular unit in the cortex of active mice. Frontiers in Cellular Neuroscience. 2015;9:17.

38. Araya R, Kudo M, Kawano M, Ishii K, Hashikawa T, Iwasato T, et al. BMP signaling through BMPRIA in astrocytes is essential for proper cerebral angiogenesis and formation of the blood-brain-barrier. Molecular and Cellular Neuroscience. 2008;38(3):417-30.

39. Marcaggi P, Attwell D. Role of glial amino acid transporters in synaptic transmission and brain energetics. Glia. 2004;47(3):217-25.

40. Araque A, Carmignoto G, Haydon PG, Oliet SHR, Robitaille R, Volterra A. Gliotransmitters Travel in Time and Space. Neuron. 2014;81(4):728-39.

41. Agulhon C, Petravicz J, McMullen AB, Sweger EJ, Minton SK, Taves SR, et al. What is the role of astrocyte calcium in neurophysiology? Neuron. 2008;59(6):932-46.

42. Hamilton NB, Attwell D. Do astrocytes really exocytose neurotransmitters? Nature Reviews Neuroscience. 2010;11(4):227-38.

43. Benfenati V, Caprini M, Dovizio M, Mylonakou MN, Ferroni S, Ottersen OP, et al. An aquaporin-4/transient receptor potential vanilloid 4 (AQP4/TRPV4) complex is essential for cell-volume control in astrocytes. Proceedings of the National Academy of Sciences of the United States of America. 2011;108(6):2563-8.

44. Brown AM, Ransom BR. Astrocyte glycogen and brain energy metabolism. Glia. 2007;55(12):1263-71.

45. Powell EM, Geller HM. Dissection of astrocyte-mediated cues in neuronal guidance and process extension. Glia. 1999;26(1):73-83.

46. Lau LW, Cua R, Keough MB, Haylock-Jacobs S, Yong VW. OPINION Pathophysiology of the brain extracellular matrix: a new target for remyelination. Nature Reviews Neuroscience. 2013;14(10):722-9.

47. Carulli D, Rhodes KE, Brown DJ, Bonnert TP, Pollack SJ, Oliver K, et al. Composition of perineuronal nets in the adult rat cerebellum and the cellular origin of their components. Journal of Comparative Neurology. 2006;494(4):559-77.

48. Bye N, Carron S, Han XD, Agyapomaa D, Ng SY, Yan E, et al. Neurogenesis and Glial Proliferation Are Stimulated Following Diffuse Traumatic Brain Injury in Adult Rats. Journal of Neuroscience Research. 2011;89(7):986-1000.

49. Yoshioka N, Hisanaga SI, Kawano H. Suppression of Fibrotic Scar Formation Promotes Axonal Regeneration Without Disturbing Blood-Brain Barrier Repair and Withdrawal of Leukocytes After Traumatic Brain Injury. Journal of Comparative Neurology. 2010;518(18):3867-81.

50. Haas CA, Rauch U, Thon N, Merten T, Deller T. Entorhinal cortex lesion in adult rats induces the expression of the neuronal chondroitin sulfate proteoglycan neurocan in reactive astrocytes. Journal of Neuroscience. 1999;19(22):9953-63.

51. Jayakumar AR, Rao KVR, Panickar KS, Moriyama M, Reddy PVB, Norenberg MD. Trauma-induced cell swelling in cultured astrocytes. Journal of Neuropathology and Experimental Neurology. 2008;67(5):417-27.

52. Rao KVR, Reddy PVB, Curtis KM, Norenberg MD. Aquaporin-4 Expression in Cultured Astrocytes after Fluid Percussion Injury. Journal of Neurotrauma. 2011;28(3):371-81.

53. Jayakumar AR, Tong XY, Ruiz-Cordero R, Bregy A, Bethea JR, Bramlett HM, et al. Activation of NF-kappa B Mediates Astrocyte Swelling and Brain Edema in Traumatic Brain Injury. Journal of Neurotrauma. 2014;31(14):1249-57.

54. Perez-Polo JR, Rea HC, Johnson KM, Parsley MA, Unabia GC, Xu GJ, et al. Inflammatory Consequences in a Rodent Model of Mild Traumatic Brain Injury. Journal of Neurotrauma. 2013;30(9):727-40.

55. Tate CC, Tate MC, LaPlaca MC. Fibronectin and laminin increase in the mouse brain after controlled cortical impact injury. Journal of Neurotrauma. 2007;24(1):226-30.

56. Heller Z, Wyatt J, Arnaud A, Wolchok JC. An In Vitro Impact Model for the Study of Central Nervous System Cell Mechanobiology. Cellular and Molecular Bioengineering. 2014;7(4):521-31.

57. McCarthy KD, Devellis J. PREPARATION OF SEPARATE ASTROGLIAL AND OLIGODENDROGLIAL CELL-CULTURES FROM RAT CEREBRAL TISSUE. Journal of Cell Biology. 1980;85(3):890-902.

58. Cahoy JD, Emery B, Kaushal A, Foo LC, Zamanian JL, Christopherson KS, et al. A transcriptome database for astrocytes, neurons, and oligodendrocytes: A new resource for understanding brain development and function. Journal of Neuroscience. 2008;28(1):264-78.

59. Fraichard A, Chassande O, Bilbaut G, Dehay C, Savatier P, Samarut J. IN-VITRO DIFFERENTIATION OF EMBRYONIC STEM-CELLS INTO GLIAL-CELLS AND FUNCTIONAL-NEURONS. Journal of Cell Science. 1995;108:3181-8.

60. Saura J. Microglial cells in astroglial cultures: a cautionary note. Journal of Neuroinflammation. 2007;4:11.

61. Bottenstein JE, Sato GH. GROWTH OF A RAT NEUROBLASTOMA CELL LINE IN SERUM-FREE SUPPLEMENTED MEDIUM. Proceedings of the National Academy of Sciences of the United States of America. 1979;76(1):514-7.

62. Tournell CE, Bergstrom RA, Ferreira A. Progesterone-induced agrin expression in astrocytes modulates glia-neuron interactions leading to synapse formation. Neuroscience. 2006;141(3):1327-38.

63. Longhi L, Saatman KE, Fujimoto S, Raghupathi R, Meaney DF, Davis J, et al. Temporal window of vulnerability to repetitive experimental concussive brain injury. Neurosurgery. 2005;56(2):364-73.

64. Laurer HL, Bareyre FM, Lee V, Trojanowski JQ, Longhi L, Hoover R, et al. Mild head injury increasing the brain's vulnerability to a second concussive impact. Journal of Neurosurgery. 2001;95(5):859-70.

65. Di Giovanni S, Movsesyan V, Ahmed F, Cernak L, Schinelli S, Stoica B, et al. Cell cycle inhibition provides neuroprotection and reduces glial proliferation and scar formation after traumatic brain injury. Proceedings of the National Academy of Sciences of the United States of America. 2005;102(23):8333-8.

66. Wilhelmsson U, Li LZ, Pekna M, Berthold CH, Blom S, Eliasson C, et al. Absence of glial fibrillary acidic protein and vimentin prevents hypertrophy of astrocytic processes and improves post-traumatic regeneration. Journal of Neuroscience. 2004;24(21):5016-21.

67. Ekmark-Lewen S, Lewen A, Israelsson C, Li GL, Farooque M, Olsson Y, et al. Vimentin and GFAP responses in astrocytes after contusion trauma to the murine brain. Restorative Neurology and Neuroscience. 2010;28(3):311-21.

68. Ellis EF, Willoughby KA, Sparks SA, Chen T. S100B protein is released from rat neonatal neurons, astrocytes, and microglia by in vitro trauma and anti-S100 increases trauma-induced delayed neuronal injury and negates the protective effect of exogenous S100B on neurons. Journal of Neurochemistry. 2007;101(6):1463-70.

69. Kamphuis W, Middeldorp J, Kooijman L, Sluijs JA, Kooi EJ, Moeton M, et al. Glial fibrillary acidic protein isoform expression in plaque related astrogliosis in Alzheimer's disease. Neurobiology of Aging. 2014;35(3):492-510.

70. Haycock JW. 3D Cell Culture: A Review of Current Approaches and Techniques. In: Haycock WJ, editor. 3D Cell Culture: Methods and Protocols. Totowa, NJ: Humana Press; 2011. p. 1-15.

71. Eucker SA, Smith C, Ralston J, Friess SH, Margulies SS. Physiological and histopathological responses following closed rotational head injury depend on direction of head motion. Experimental Neurology. 2011;227(1):79-88.

72. Cullen DK, Vernekar VN, LaPlaca MC. Trauma-Induced Plasmalemma Disruptions in Three-Dimensional Neural Cultures Are Dependent on Strain Modality and Rate. Journal of Neurotrauma. 2011;28(11):2219-33.

73. Tian J, Pecaut MJ, Slater JM, Gridley DS. Spaceflight modulates expression of extracellular matrix, adhesion, and profibrotic molecules in mouse lung. Journal of Applied Physiology. 2010;108(1):162-71.

74. Basile V, Romano G, Fusi F, Monici M. Comparison Between the Effects of Hypergravity and Photomechanical Stress on Cells Producing ECM. Microgravity Science and Technology. 2009;21(1-2):151-7.

75. Searby ND, Steele CR, Globus RK. Influence of increased mechanical loading by hypergravity on the microtubule cytoskeleton and prostaglandin E-2 release in primary osteoblasts. American Journal of Physiology-Cell Physiology. 2005;289(1):C148-C58.

76. Lwigale PY, Thurmond JE, Norton WN, Spooner BS, Wiens DJ. Simulated microgravity and hypergravity attenuate heart tissue development in explant culture. Cells Tissues Organs. 2000;167(2-3):171-83.

77. McCann MR, Patel P, Beaucage KL, Xiao YZ, Bacher C, Siqueira WL, et al. Acute Vibration Induces Transient Expression of Anabolic Genes in the Murine Intervertebral Disc. Arthritis and Rheumatism. 2013;65(7):1853-64.

78. Bottlang M, Sommers MB, Lusardi TA, Miesch JJ, Simon RP, Xiong ZG. Modeling neural injury in organotypic cultures by application of inertia-driven shear strain. Journal of Neurotrauma. 2007;24(6):1068-77.

79. Floyd CL, Gorin FA, Lyeth BG. Mechanical strain injury increases intracellular sodium and reverses Na+/Ca2+ exchange in cortical astrocytes. Glia. 2005;51(1):35-46.

80. Zhao XR, Ahram A, Berman RF, Muizelaar JP, Lyeth BG. Early loss of astrocytes after experimental traumatic brain injury. Glia. 2003;44(2):140-52.

81. Staffa K, Ondruschka B, Franke H, Dressler J. Cerebellar Gene Expression following Human Traumatic Brain Injury. Journal of Neurotrauma. 2012;29(17):2716-21.

82. Cobb JA, O'Neill K, Milner J, Mahajan GJ, Lawrence TJ, May WL, et al. DENSITY OF GFAP-IMMUNOREACTIVE ASTROCYTES IS DECREASED IN LEFT HIPPOCAMPI IN MAJOR DEPRESSIVE DISORDER. Neuroscience. 2016;316:209-20.

83. Nagy C, Suderman M, Yang J, Szyf M, Mechawar N, Ernst C, et al. Astrocytic abnormalities and global DNA methylation patterns in depression and suicide. Molecular Psychiatry. 2015;20(3):320-8.

84. Ahman S, Saveman BI, Styrke J, Bjornstig U, Stalnacke BM. LONG-TERM FOLLOW-UP OF PATIENTS WITH MILD TRAUMATIC BRAIN INJURY: A MIXED-METHODS STUDY. Journal of Rehabilitation Medicine. 2013;45(8):758-64.

85. Guskiewicz KM, McCrea M, Marshall SW, Cantu RC, Randolph C, Barr W, et al. Cumulative effects associated with recurrent concussion in collegiate football players - The NCAA Concussion Study. Jama-Journal of the American Medical Association. 2003;290(19):2549-55.

86. Slemmer JE, Matser EJT, De Zeeuw CI, Weber JT. Repeated mild injury causes cumulative damage to hippocampal cells. Brain. 2002;125:2699-709.

87. Shultz SR, Bao F, Omana V, Chiu C, Brown A, Cain DP. Repeated Mild Lateral Fluid Percussion Brain Injury in the Rat Causes Cumulative Long-Term Behavioral Impairments, Neuroinflammation, and Cortical Loss in an Animal Model of Repeated Concussion. Journal of Neurotrauma. 2012;29(2):281-94.

88. Heck N, Garwood J, Dobbertin A, Calco V, Sirko S, Mittmann T, et al. Evidence for distinct leptomeningeal cell-dependent paracrine and EGF-linked autocrine regulatory pathways for suppression of fibrillar collagens in astrocytes. Molecular and Cellular Neuroscience. 2007;36(1):71-85.

89. Vogelaar CF, König B, Krafft S, Estrada V, Brazda N, Ziegler B, et al. Pharmacological Suppression of CNS Scarring by Deferoxamine Reduces Lesion Volume and Increases Regeneration in an <italic>In Vitro</italic> Model for Astroglial-Fibrotic Scarring and in Rat Spinal Cord Injury <italic>In Vivo</italic>. PLoS ONE. 2015;10(7):e0134371.

90. Harris NG, Carmichael ST, Hovda DA, Sutton RL. Traumatic Brain Injury Results in Disparate Regions of Chondroitin Sulfate Proteoglycan Expression That Are Temporally Limited. Journal of Neuroscience Research. 2009;87(13):2937-50.

91. Reeves TM, Prins ML, Zhu JP, Povlishock JT, Phillips LL. Matrix metalloproteinase inhibition alters functional and structural correlates of deafferentation-induced sprouting in the dentate gyrus. Journal of Neuroscience. 2003;23(32):10182-9.

92. Sullivan KE, Quinn KP, Tang KM, Georgakoudi I, Black LD. Extracellular matrix remodeling following myocardial infarction influences the therapeutic potential of mesenchymal stem cells. Stem Cell Research & Therapy. 2014;5:15.

93. Pellitteri R, Catania MV, Bonaccorso CM, Ranno E, Dell'Albani P, Zaccheo D. Viability of olfactory ensheathing cells after hypoxia and serum deprivation: Implication for therapeutic transplantation. Journal Of Neuroscience Research. 2014;92(12):1757-66.

94. Puschmann TB, Turnley AM. Eph receptor tyrosine kinases regulate astrocyte cytoskeletal rearrangement and focal adhesion formation. Journal of Neurochemistry. 2010;113(4):881-94.

95. Maneshi MM, Sachs F, Hua SSZ. A Threshold Shear Force for Calcium Influx in an Astrocyte Model of Traumatic Brain Injury. Journal of Neurotrauma. 2015;32(13):1020-9.

96. Du S, Rubin A, Klepper S, Barrett C, Kim YC, Rhim HW, et al. Calcium influx and activation of Calpain I mediate acute reactive gliosis in injured spinal cord. Experimental Neurology. 1999;157(1):96-105.

97. Nilius B, Vriens J, Prenen J, Droogmans G, Voets T. TRPV4 calcium entry channel: a paradigm for gating diversity. American Journal of Physiology-Cell Physiology. 2004;286(2):C195-C205.

98. O'Conor CJ, Leddy HA, Benefield HC, Liedtke WB, Guilak F. TRPV4-mediated mechanotransduction regulates the metabolic response of chondrocytes to dynamic loading. Proceedings of the National Academy of Sciences of the United States of America. 2014;111(4):1316-21.

## VI. Tables and Figures

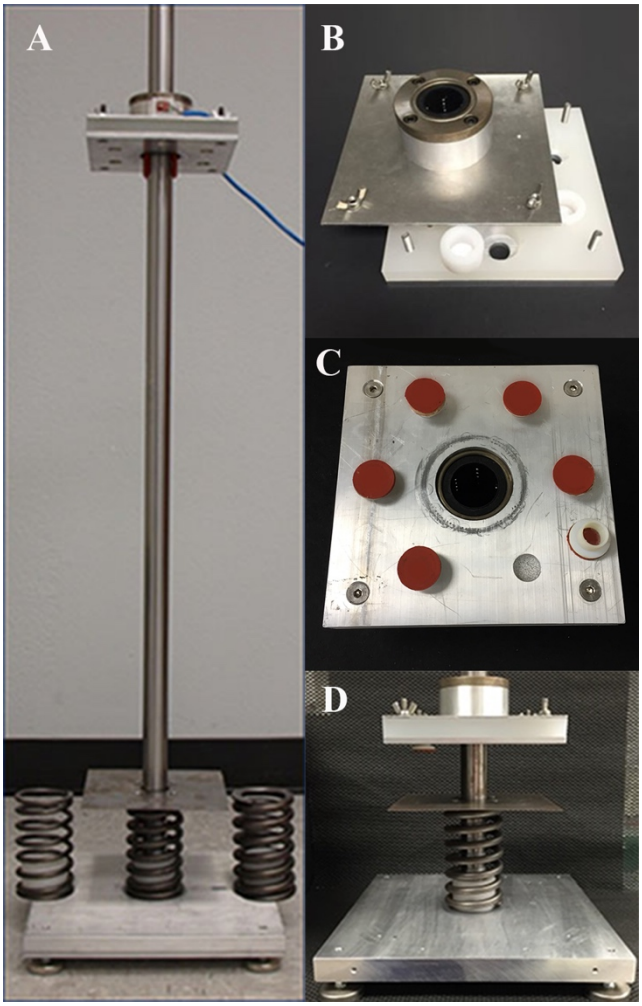


**Figure 1.** Bioreactor capable of implementing mechanical stimuli mimicking a traumatic brain injury. The bioreactor is comprised of four main components: The guide rod (A) constricts the motion of the bioreactor to the vertical direction. The drop shuttle (B) comprises of two aluminum plates sandwiching a polypropylene layer. The bottom aluminum plate of the drop shuttle has six openings for custom made acrylic inserts that apply up to 30% biaxial strain to cultures (C). A steel plate mounted onto an interchangeable spring creates a spring dampened impact base prolonging the inertial forces felt by cell cultures (D).

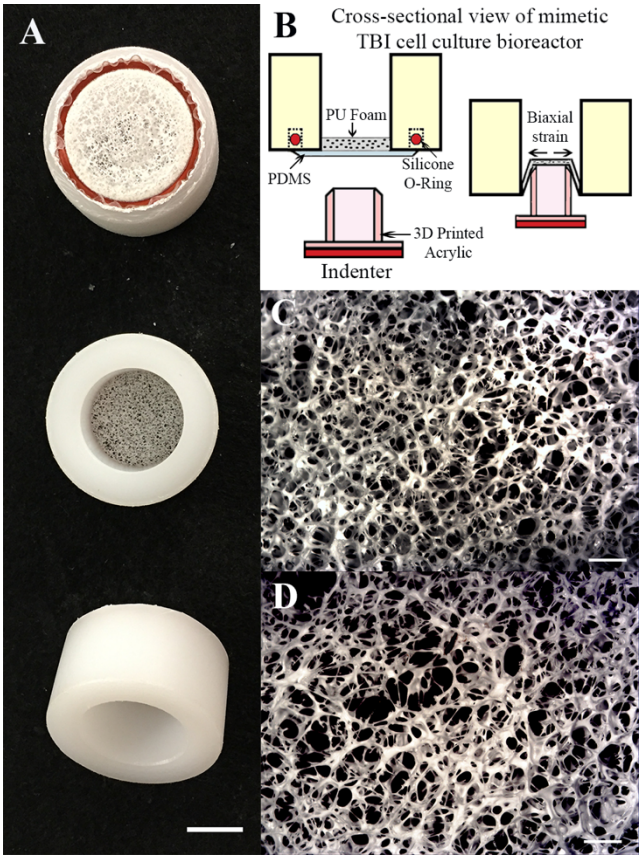


**Figure 2**. Fabricated cell culture drums compatible with the mimetic traumatic brain injury bioreactor. Cell culture drums are fabricated by creating a porous three-dimensional polyurethane foam and securing the foam to the base of a polypropylene cylinder (A). Biaxial strain can be applied to the cell culture by inserting an acrylic indenter into the elastic cell culture (B). The porous polyurethane foam exhibits elastic behavior at low strains and is shown at a relaxed and stretched state (C,D). Scale bars are representative as follows: Panel A – 1 cm, Panels C, D – 1 mm.

**Table 1. Comparing bioreactor characteristics for three spring dampened bases**

| Spring | Spring Constant (lbs $in^{-1}$) | Impact Duration (ms) | Peak Deceleration (G) | Sensitivity (G $cm^{-1}$) | $R^2$ |
|---|---|---|---|---|---|
| Stiff | 959 | 1.6 ± 0.3 | 184.5 ± 26.6 | 0.726 | 0.947 |
| Medium | 312 | 9.2 ± 1.2 | 158.2 ± 28.8 | 0.734 | 0.972 |
| Flexible | 90 | 19.3 ± 0.5 | 59.1 ± 4.3 | 0.213 | 0.947 |

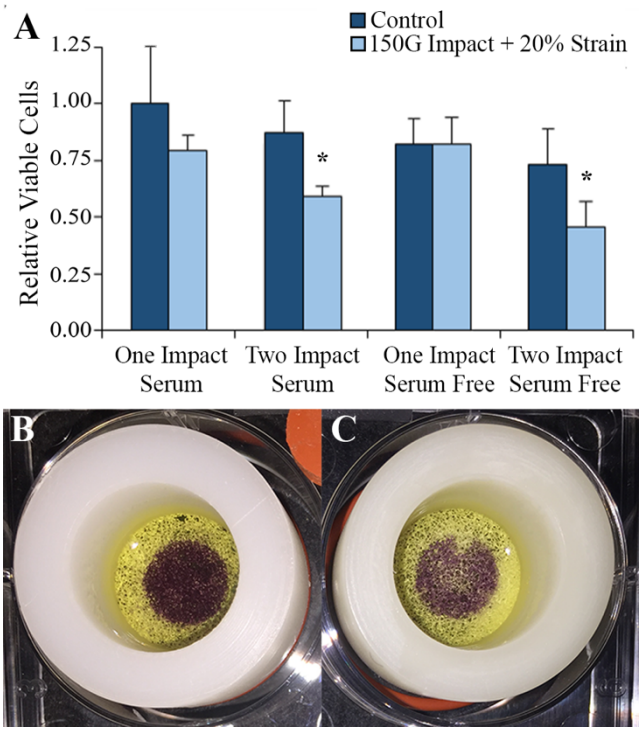


**Figure 3.** Relative cell viability for astrocytes 24 hours following mimetic traumatic brain injury. A modified MTT Assay quantified the short term cell survival for astrocytes cultured with and without 10% fetal bovine serum following one or two TBI mimetic impacts. Impacted cultures were made relative to the single impact, serum containing media control (A). Withholding serum containing media and stimulating astrocytes with one or two TBI-like impacts decreased astrocyte survival compared to controls. MTT precipitates for controls (B) indicate strong astrocyte presence located within the seeding zone and little outgrowth into the surrounding scaffold. Lack of precipitation for impacted cultures (C) demonstrate areas with lowered cell density. * decrease from control ($p<0.05$), n=6, mean ± SEM.

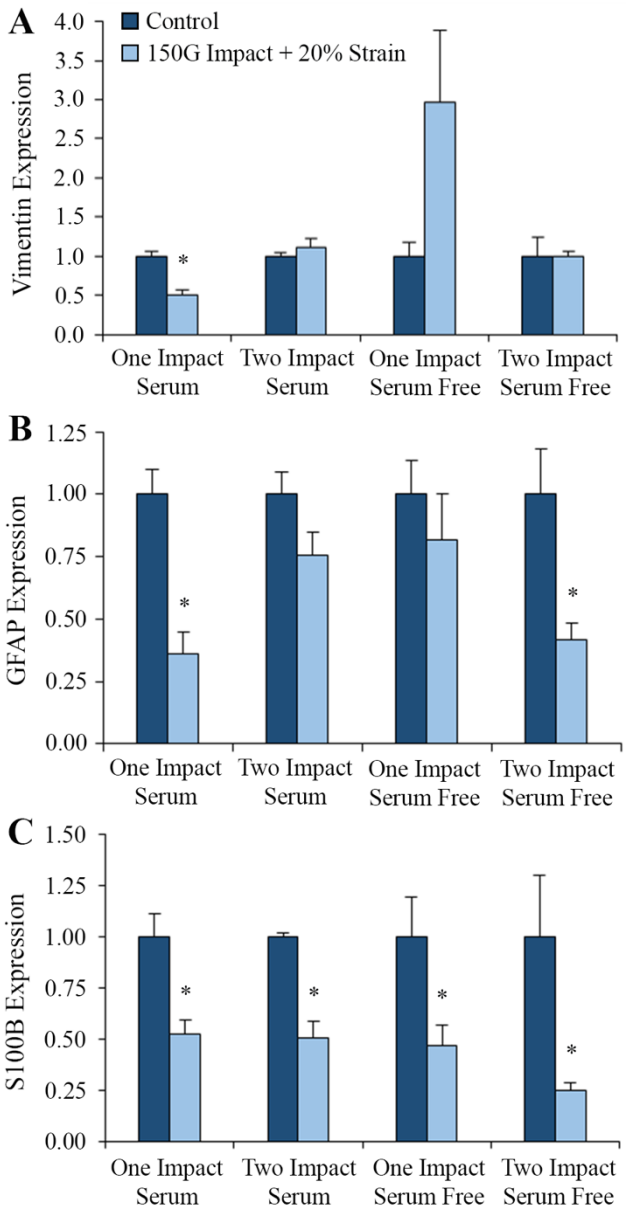


**Figure 4.** Expression for common markers for reactive gliosis in astrocytes decreased 24 hours after mechanical stimulation. Vimentin expression (A) was reduced in single impact, serum containing media cultures, but remained unchanged in all other conditions. Surprisingly, GFAP expression (B), a hallmark of reactive gliosis, was suppressed in all experimental conditions, though only significantly in single impact serum containing conditions and two impact serum withheld conditions. Additionally, S100B expression (C) was decreased across all experimental conditions. *significant difference from the control group ($p<0.05$), n=4-5, mean ± SEM.

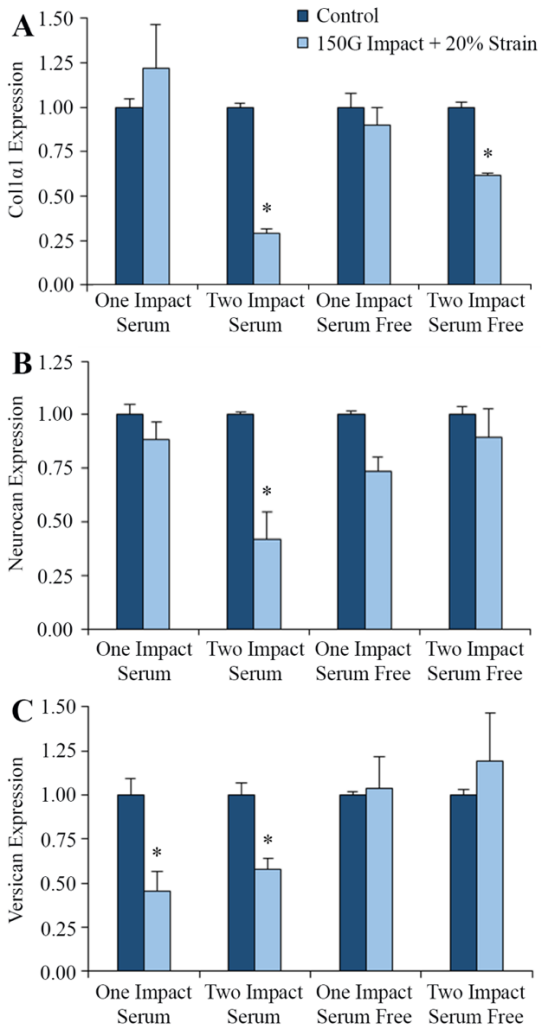


**Figure 5.** Astrocyte gene expression for structural extracellular matrix proteins Collagen I (A), Neurocan (B), and Versican (C) six hours after mimetic TBI. Expression levels for each sample group are relative to the control of that group and normalized to the housekeeping gene GAPDH. Astrocytes cultured in serum containing media and given two mimetic TBIs separated by 24 hours decreased expression of all ECM proteins tested. Additionally, collagen I expression was decreased in astrocyte cultures receiving two impacts, no matter the media. Versican expression was decreased in impacted astrocyte cultured in serum containing media. * significant difference from control group ($p<0.05$), n=4, mean ± SEM.

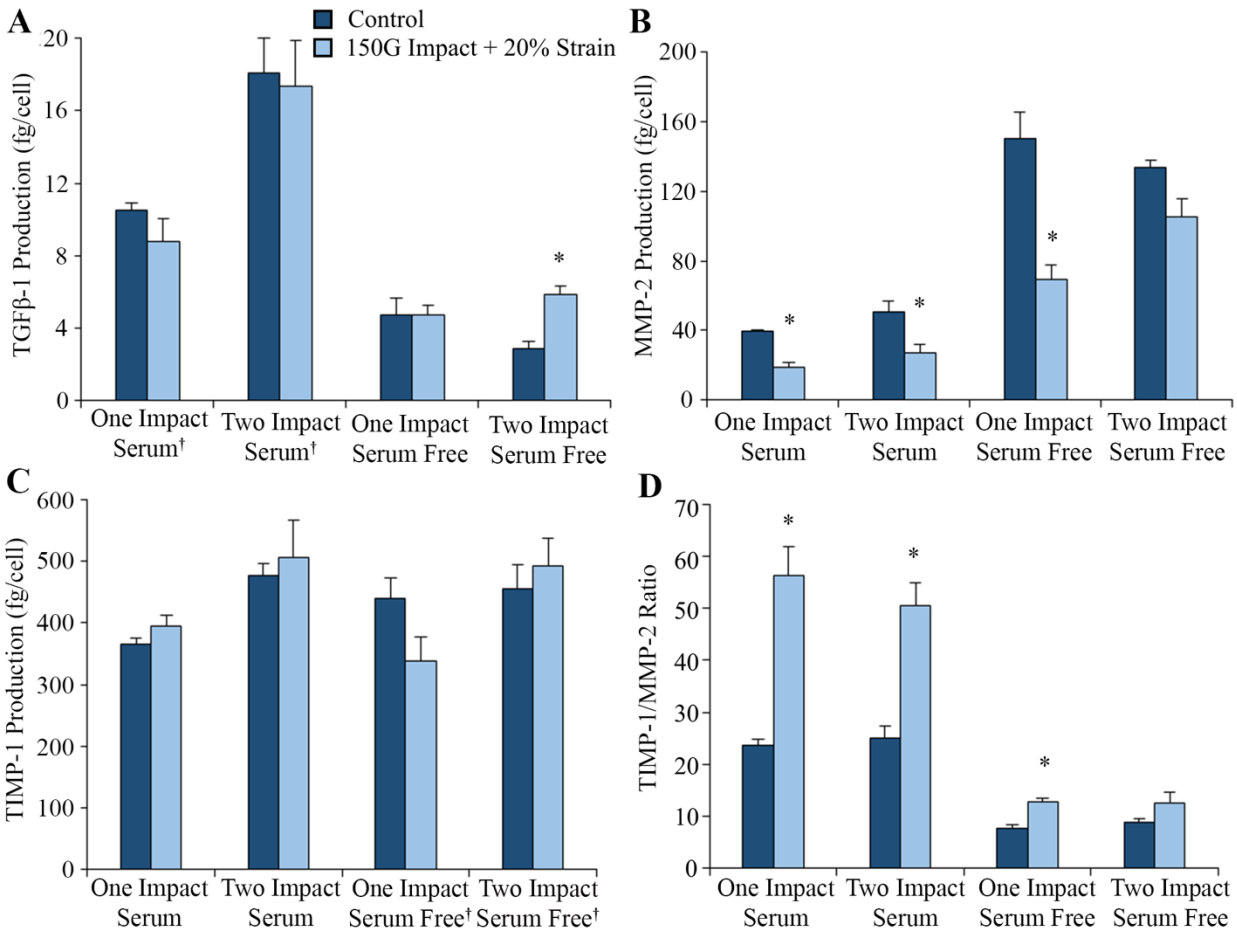


**Figure 6.** Collection of astrocyte protein secretions for Matrix Metalloproteinase 2 (A), Tissue inhibitor of metalloproteinases 1 (B), and Transforming Growth Factor Beta 1 (C) 48 hours after mimetic TBI. Cell culture supernatants were collected 48 hours following the final impact for each treatment group. Protein concentrations were quantified using a colormetric sandwich ELISA kit. Concentrations were normalized to the viable cell counts reported previously. The ratio of the production of TIMP-1 to MMP-2 production (D) indicates an inhibition in the breakdown of ECM. * significant difference from control group ($p<0.05$), n=4, mean ± SEM.

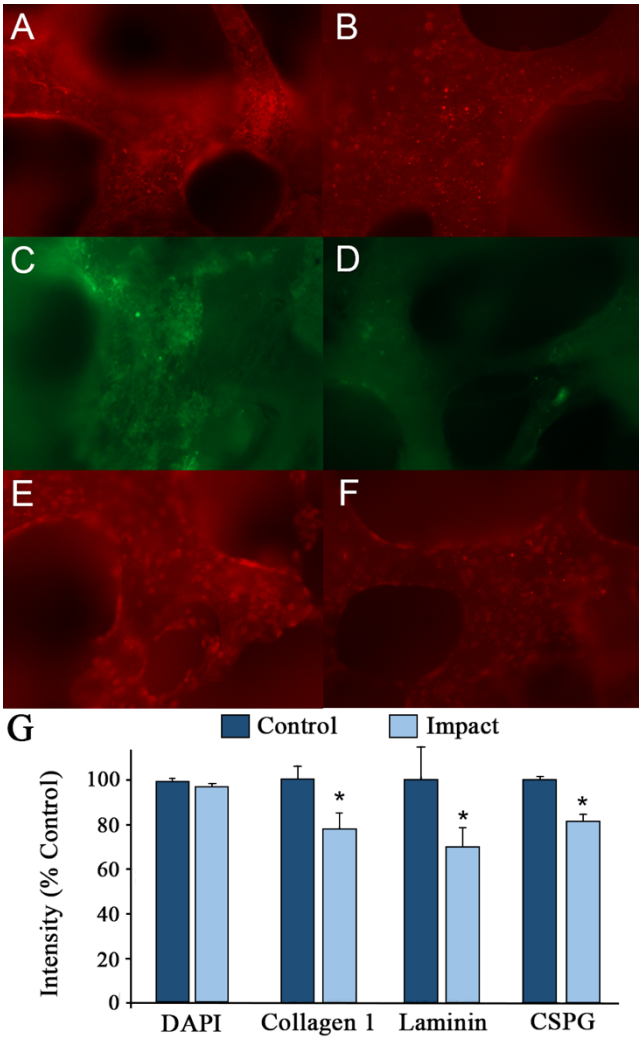


**Figure 7.** Representative microscopic (100X) images of matrix protein accumulation and distribution after three weeks in culture for control and impacted scaffolds showing immunoreactivity for collagen type I (A&B), laminin (C&D), and CSPG (E&F). Quantitative analysis of extracellular matrix accumulation after three weeks for control and impacted scaffolds expressed as a percentage of the controls (G) showing that immunoreactivity against both collagen type I, and laminin CSPG was significantly reduced (* = t-test, $p<0.05$) in the impacted group when compared to static controls (mean ± SD, N =6/sample group).

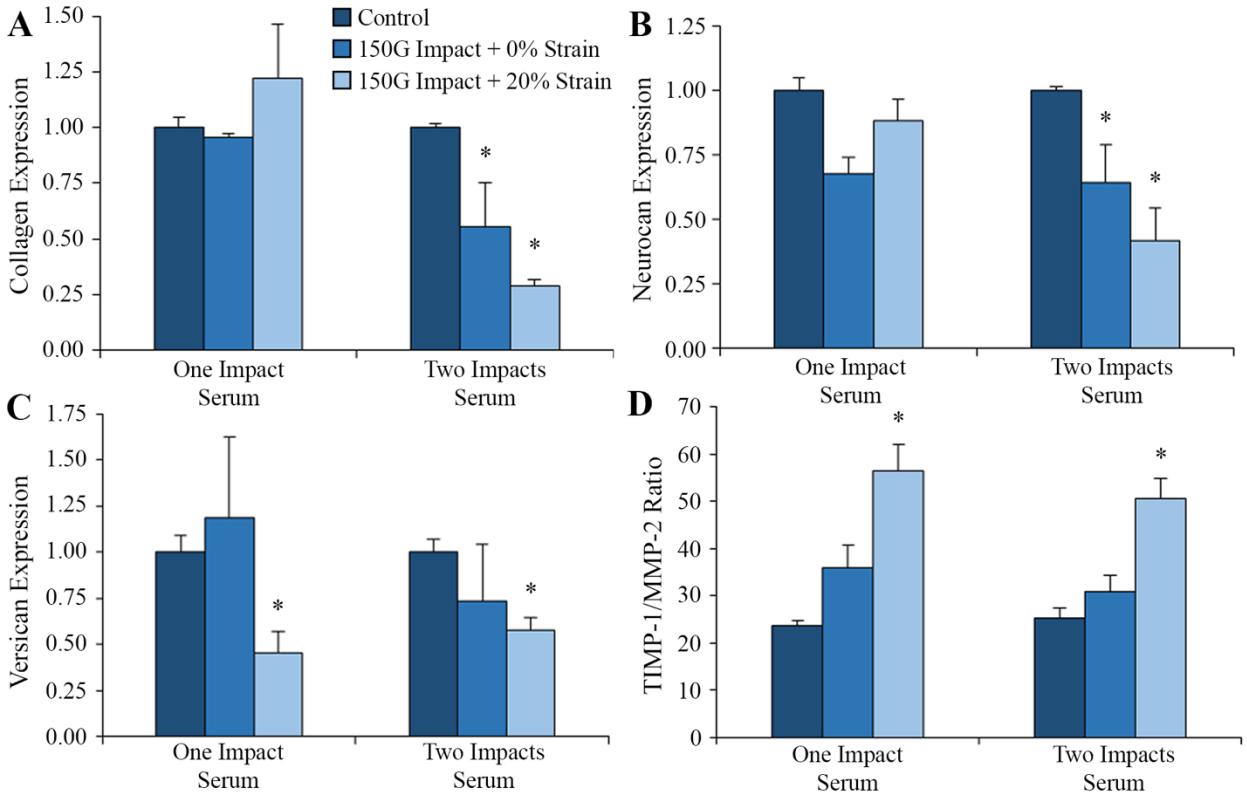


**Supplemental Figure 1.** Inertial loading without stain on astrocytes resulted in middling expression levels for extracellular matrix proteins. Collagen I expression (A) and neurocan expression (B) were significantly reduced in cultures receiving two 150G impacts without biaxial strain compared to controls, though not as suppressed as cultures receiving two 150G impacts with biaxial strain. Versican expression (C) displayed a similar trend in two impact conditions though was not significant. The ratio of TIMP-1 to MMP-2 (D) found in the media 48 hours after impact without strain exhibited middling behavior between the control and impact with strain groups. Error bars are representative of SEM. Asterisks are indicative of significant difference from the control ($p<0.05$).

## VII. Appendix A: Validating Astrocyte Purity through Image Processing

The most common cell type used in studying astrocytes in the literature are primary cultures isolated from neonatal rat pup cortices. The initial dissociation step results in a culture of mixed central nervous system cells containing neurons, oligodendrocytes, microglia, and astrocytes. To isolate astrocytes, a series of shaking steps are performed as astrocytes will adhere strongly to tissue culture plastic while other central nervous system cells adhere loosely. After shaking, cultures are passaged with some cells being plated onto coverslips for validation of the purity of the astrocyte culture. To use in downstream experiments, the user must first validate 90% of cells in the primary culture are astrocytes and are expressing GFAP, an established marker for astrocytes.

Cells cultured on coverslips are incubated 1-2 days, fixed, and stained using a fluorescent marker for GFAP (indirect immunofluorescence staining) and cell nuclei (DAPI). The coverslips are imaged using fluorescent microscopy obtaining images of cell nuclei and GFAP at the same locations within the coverslip. Multiple images are obtained from each cover slip (4-5 images, use 5-6 cover slips). Images are loaded into a single folder and processed through a series of custom-built Matlab functions.

The number of cells in the image is calculated using watershed segmentation of the DAPI image. First, the DAPI image is converted to grayscale and enhanced by stretching the contrast across the dynamic range such that 50% of the pixels have a value of 0 and 1% of the pixels are saturated. Any nuclei touching the edges of the image are discounted. A Gaussian filter is applied to the image to eliminate local maxima within nuclei. Otsu's method converts the grayscale image into a binary mask by setting a gray level threshold value that sends all pixels below the threshold to 0 and all pixels above the threshold to saturation. The threshold value is

determined by minimizing intragroup variation and maximizing intergroup variation. The binary mask is opened to eliminate small artifacts stemming from debris that are not corresponding to cells. The mask is applied to the enhanced DAPI image and the local maximum is found within each cell. The local maximum is isolated and dilated. Inverting the DAPI image with the dilated local maximum creates nuclei with deep 'wells' to improve the performance of watershed segmentation. Finally, watershed segmentation isolates individual nuclei and the built in Matlab function bwlabel outputs the number of cells in the image. In determining if the cell is GFAP positive, a mask is created around each cell nuclei from the DAPI image. The GFAP image is applied to the mask and the average intensity of the GFAP signal surrounding the nuclei is determined. If it is greater than the background signal, it is determined that the cell is expressing GFAP and can be counted as an astrocyte. In all experiments, cell cultures must contain a minimum of 90% GFAP positive cells.

## VIII. Appendix B: Next Generation TBI Bioreactor

One can argue that the elastic foam used to culture astrocytes in the traumatic brain injury bioreactor is not an accurate representation of the extracellular environment. To this end, modifications to the original device were performed to create an injury model better representing an insult that would lead to TBI (Figure A1). The modifications are summarized below:

- Adding a second polypropylene plate to increase the space above the astrocyte culture
- Replacing the polyurethane foam as a cell substrate by casting astrocytes in an alginate hydrogel or Matrigel
- Removing the biaxial stretch injury indenter
- Adding a Teflon weight that can carry additional stainless steel weights to control the mass compressing the gel
- Exchanging the spring base with a foam base to increase impact duration and create a smooth impact profile

The modifications improve the design of the bioreactor by first culturing cells in an environment better representing of the soft meshwork of extracellular proteins that make up the central nervous system. By using a weight to compress the gels, the cells are subject to the deceleration of the fall, pressure generated by the weight upon deceleration, and stretching as the gel deforms outwardly to fill the bottom of the cell culture drum in response to the pressure. The device has been characterized to determine peak decelerations over varying heights at 25cm increments (Figure A2). Adjusting the weight allows the user to control the pressure applied to the gel by Newton's Second Law (Eq. 1) and the definition of pressure (Eq. 2).

$$F = ma \qquad \text{(Eq. 1)}$$

$$P = \frac{F}{A} \tag{2}$$

$$P = \frac{ma}{A} \tag{3}$$

Peak pressures can be matched to physiological conditions experienced in the brain during an impact causing TBI. The flexibility of controlling the weight allows the user to investigate the effects of acceleration and pressure individually. Exchanging the spring base with a foam base created a smooth bell shaped impact profile similar to that previously reported in the literature (Figure A2). This is advantageous as the steel plate of the spring base expressed a rapid peak in deceleration that could be described as a jolt that could be inconsistent between drops.

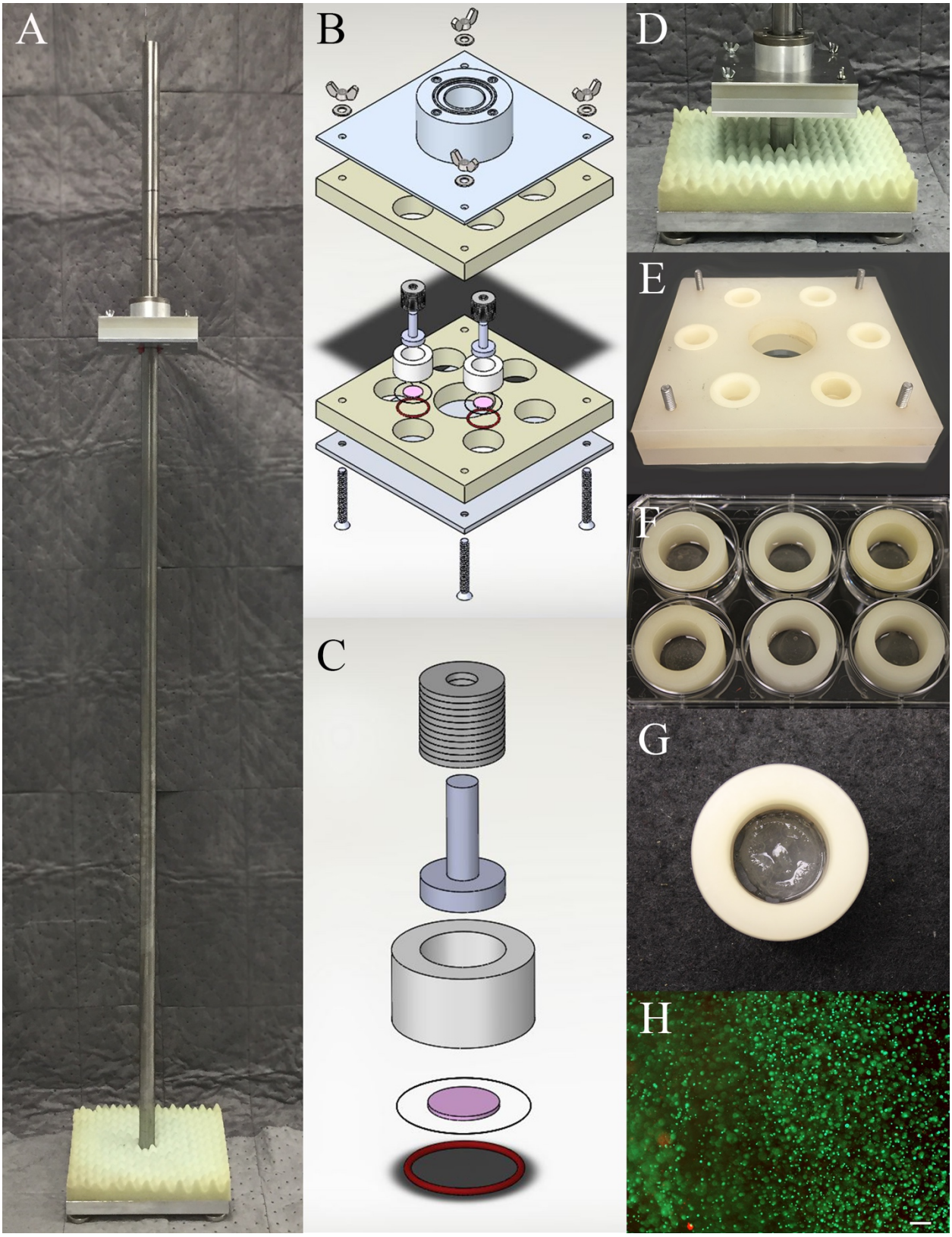
A
B
C
D
E
F
G
H

**Figure B1.** Next Generation TBI Bioreactor. The bioreactor consists of an aluminum guide rod press fit into an aluminum base (A). The design of the shuttle includes two aluminum plates sandwiching two polypropylene plates with six holes cut out to house cell cultures (B). Cells are cultured in a polypropylene drum using PDMS as a base secured by a silicone O-ring (C). Cell cultures are injured using a Teflon weight placed on top of the culture that compresses the cultures upon impact. The weight can be adjusted by adding stainless steel rings onto the top of the weight. The base of the drop structure has been modified to have an egg crate base to create smooth loading and unloading curves. The shuttle can house six separate cultures (E). Astrocytes are cast into alginate gels (F,G) and are viable within the gels after 96 hours as determined by the fluorescent marker calcein (H). Scale bar is representative of 100 μm.

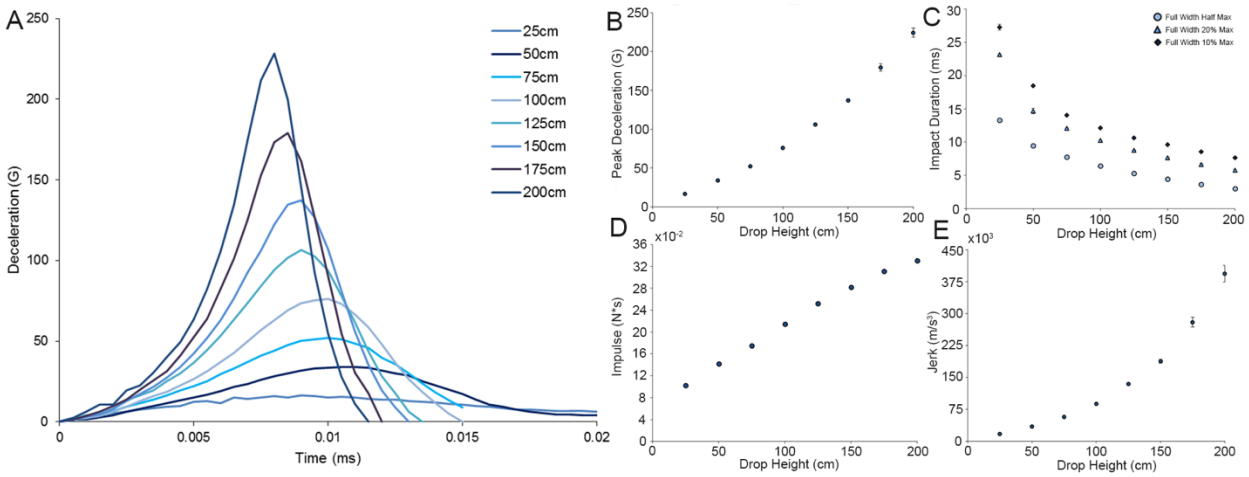


**Figure B2.** Characterization of Next Gen TBI Bioreactor. Representative curves of eight different drop heights display physiologically relevant deceleration profiles (A). The average peak deceleration at each drop height (n=10) established a quadratic relationship between drop height and peak deceleration (B). The full width half max, full width 20% max, and full width 10% max describe the impact duration (C). The impulse is a measure of change of momentum and was calculated as the area under the acceleration curve multiplied by the maximum weight used in the bioreactor (0.383 g) (D). Jerk is the rate of change in acceleration and is calculated as the change in acceleration from the initial time point to the peak deceleration (E).

## IX. Appendix C: TRPV4-Mediated Calcium Signaling

Investigating pathways that astrocytes sense and respond to mechanical forces inducing an injury response is a future goal for our research group. One potential pathway to investigate is through the mechanically-sensitive calcium channel TRPV4(97). Chondrocytes respond to cyclical compression *in vitro* through the TRPV4 channel increasing extracellular matrix production and altering the mechanical and chemical properties of ECM(98). Knowing the modulations astrocytes perform in the CNS after insult, we hypothesize that the TRPV4 channel acts as a mechanotransducer in astrocytes presenting a pathway to sense injury and invoke a calcium response that triggers an injury cascade. As an initial step, we sought to discover if activating TRPV4 triggers an inflammatory response or altered extracellular matrix protein production in astrocytes. As an initial step, a dose response to a chemical agonist, GSK101 (Sigma Aldrich) was performed to determine concentrations required to invoke a cellular response. Intracellular calcium concentrations were measured using calcium sensitive Fura-2 dye. Briefly, astrocytes were seeded onto laminin-coated coverslips and incubated until cells reached confluency. Cells were rinsed with PBS and incubated in Fura-2 AM (Molecular Probes) for 30 minutes at room temperature. Cells were again rinsed in PBS and incubated in Tyrode's Buffer (Sigma Aldrich) for 15 minutes at room temperature. Fresh Tyrode's buffer was added prior to imaging. Cells (n=5) were imaged on an inverted microscope (Motic AE31) with emitted light captured using a photomultiplier (IonOptix) from excitation wavelengths of 340nm and 380nm sampling at 500Hz. Cultures were imaged for 60 seconds to create a baseline. GSK101 was introduced at varying concentrations at the 60 second time point and calcium influx was recorded over the following 440 seconds. Traces were reported as the ratio of emission from 340nm to 380nm excitation wavelengths with increases in this ratio corresponding to an influx of calcium into the

cell. The baseline ratio subtracted from the peak 340nm/380nm ratio and normalized to the baseline provided a unitless measure to compare the calcium response to the introduction of the agonist. Overall, a trend of increased intracellular calcium concentrations is observed in response to higher concentrations of GSK101 (Figure B1). However, a one-way ANOVA did not show significant differences between any treatment groups. Large variances within treatment groups likely prevented a significant result to be observed.

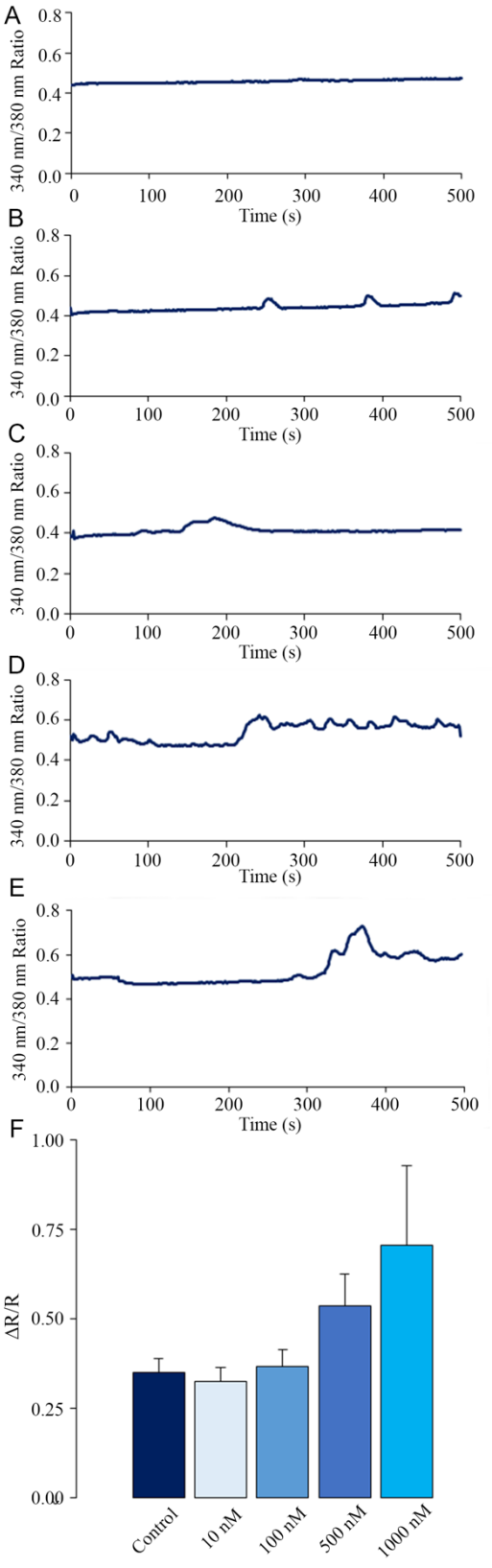
A
B
C
D
E
F
340 nm/380 nm Ratio
Time (s)
0.0
0.2
0.4
0.6
0.8
0
100
200
300
400
500
ΔR/R
0.00
0.25
0.50
0.75
1.00
Control
10 nM
100 nM
500 nM
1000 nM

**Figure C1.** Calcium Influx in Astrocytes in Response to TRPV-4 Agonist. Representative curves of the ratio of emission when excited at 340nm and 380nmfor astrocytes treated with a TRPV4 agonist GSK101 at 0nM (A), 10nM (B), 100nM (C), 500nM (D), and 1000nM (E). Increases to the 340nm/380nm corresponds to intracellular increases in calcium stemming from the opening of the calcium channel TRPV4. The average difference between the peak 340nm/380nm ratio and baseline ratio was normalized to the baseline ratio for each culture (n=5/concentration) (F). Error bars are representative of SEM.

# X. Appendix D: IACUC Protocol Approval #15013

UNIVERSITY OF ARKANSAS

Office of Research Compliance

MEMORANDUM

TO: Dr. Jeffrey Wolchok

FROM: Craig N. Coon, Chairman
Institutional Animal Care and Use Committee (IACUC)

DATE: October 13, 2014

SUBJECT: IACUC APPROVAL
Expiration date: 10-14-2017

The Institutional Animal Care and Use Committee (IACUC) has APPROVED your protocol 15013: *'Exploring Astrocyte Mechanobiology'* beginning 10-15-14

In granting its approval, the IACUC has approved only the information provided. Should there be any further changes to the protocol during the research, please notify the IACUC in writing(via the Modification form) prior to initiating the changes. If the study period is expected to extend beyond 10-14-2017 you must submit a new protocol prior to that date to avoid any interruption. By policy the IACUC cannot approve a study for more than 3 years at a time.

The IACUC appreciates your cooperation in complying with University and Federal guidelines involving animal subjects.

CNC/aem

cc: Animal Welfare Veterinarian

Administration Building 210 • 1 University of Arkansas • Fayetteville, AR 72701-1201 • 479-575-4572
Fax: 479-575-3846 • http://vpred.uark.edu/199